Atmos. Chem. Phys. Discuss., 11, 33583–33650, 2011
www.atmos-chem-phys-discuss.net/11/33583/2011/
doi:10.5194/acpd-11-33583-2011

Atmospheric Chemistry and Physics Discussions

DO_3SE modelling of soil moisture to determine ozone flux to European forest trees

P. Büker [1], T. Morrissey [1], A. Briolat [1], R. Falk [1], D. Simpson [2,3], J.-P. Tuovinen [4], R. Alonso [5], S. Barth [6], M. Baumgarten [7], N. Grulke [8], P. E. Karlsson [9], J. King [10,11], F. Lagergren [12], R. Matyssek [7], A. Nunn [7], R. Ogaya [13], J. Peñuelas [13], L. Rhea [10], M. Schaub [14], J. Uddling [6], W. Werner [15], and L. D. Emberson [1]

[1]Stockholm Environment Institute at York, Environment Department, University of York, York, UK
[2]EMEP MSC-W, Norwegian Meteorological Institute, Oslo, Norway
[3]Department of Radio & Space Science, Chalmers University of Technology, Gothenburg, Sweden
[4]Finnish Meteorological Institute, Helsinki, Finland
[5]Ecotoxicology of Air Pollution, CIEMAT, Madrid, Spain
[6]Department of Plant and Environmental Sciences, University of Gothenburg, Gothenburg, Sweden
[7]Department of Ecology and Ecosystem Management, Life Science Center Weihenstephan, Technische Universität München, Freising, Germany

[8]Western Wildlands Environmental Threats Assessment Center, USDA Forest Service, Pacific Northwest Research Station, Prineville, Oregon, USA
[9]IVL, Swedish Environmental Research Institute, Gothenburg, Sweden
[10]Department of Forestry and Environmental Resources, North Carolina State University, Raleigh, USA
[11]Department of Biology, University of Antwerp, Wilrijk, Belgium
[12]Department of Physical Geography, Lund University, Lund, Sweden
[13]Global Ecology Unit CREAF-CEAB-CSIC, CREAF (Center for Ecological Research and Forestry Applications), Universitat Autònoma de Barcelona, Barcelona, Spain
[14]Swiss Federal Research Institute WSL, Birmensdorf, Switzerland
[15]Department of Geobotany, University Trier, Trier, Germany

Received: 30 September 2011 – Accepted: 2 December 2011 – Published: 20 December 2011

Correspondence to: P. Büker (patrick.bueker@sei-international.org)

Published by Copernicus Publications on behalf of the European Geosciences Union.

ACPD
11, 33583–33650, 2011

Abstract

The DO_3SE (Deposition of O_3 for Stomatal Exchange) model is an established tool for estimating ozone (O_3) deposition, stomatal flux and impacts to a variety of vegetation types across Europe. It has been embedded within the EMEP (European Monitoring and Evaluation Programme) photochemical model to provide a policy tool capable of relating the risk of vegetation damage to O_3 precursor emission scenarios for use in policy formulation. A key limitation of regional flux-based risk assessments so far has been the approximation that soil water deficits are not limiting O_3 flux due to the unavailability of evaluated methods for modelling soil water deficits and their influence on stomatal conductance (g_{sto}), and ultimately O_3 flux.

This paper describes the development and evaluation of a method to estimate soil moisture status and its influence on g_{sto} for a variety of forest tree species. The soil moisture module uses the Penman-Monteith energy balance method to drive water cycling through the soil-plant-atmosphere system and empirical data describing g_{sto} relationships with pre-dawn leaf water status to estimate the biological control of transpiration. We trial four different methods to estimate this biological control of the transpiration stream, which vary from simple methods that relate soil water content or potential directly to g_{sto} to more complex methods that incorporate hydraulic resistance and plant capacitance that control water flow through the plant system.

These methods are evaluated against field data describing a variety of soil water variables, g_{sto} and transpiration data for Norway spruce (*Picea abies*), Scots pine (*Pinus sylvestris*), birch (*Betula pendula*), aspen (*Populus tremuloides*), beech (*Fagus sylvatica*) and holm oak (*Quercus ilex*) collected from ten sites across Europe and North America. Modelled estimates of these variables show consistency with observed data when applying the simple empirical methods, with the timing and magnitude of soil drying events being captured well across all sites and reductions in transpiration with the onset of drought being predicted with reasonable accuracy. The more complex methods which incorporate hydraulic resistance and plant capacitance perform less

ACPD

11, 33583–33650, 2011

well, with predicted drying cycles consistently underestimating the rate and magnitude of water lost from the soil.

A sensitivity analysis showed that model performance was strongly dependent upon the local parameterisation of key model drivers such as the maximum stomatal conductance, soil texture, root depth and leaf area index. The results suggest that the simple modelling methods that relate g_{sto} directly to soil water content and potential provide adequate estimates of soil moisture and influence on g_{sto} such that they are suitable to be used to assess the potential risk posed by O_3 to forest trees across Europe.

1 Introduction

Ground level ozone (O_3) is an important air pollutant and greenhouse gas that has been found to affect forest trees through visible injury (Schaub et al., 2010; Novak et al., 2005); changes in plant physiology and carbon allocation (Novak et al., 2007); acceleration of leaf senescence (Bussotti et al., 2011); predisposition of trees to attacks by pests and pathogens (Manning and von Tiedemann, 1995); decreasing growth, productivity and fitness of forests (Matyssek and Sandermann, 2003; Karnosky et al., 2007; Matyssek et al., 2010a,b) with possible consequences for altered carbon sequestration potentials of forest ecosystems (Sitch et al., 2007; Bytnerowicz et al., 2007). Current O_3 levels across Europe are considered high enough to constitute a risk for forests across the region with further implications for agro-forestry, renewable resource management and post-Kyoto policies (Matyssek et al., 2008; Mills et al., 2011). The development of metrics to define O_3 exposure in relation to plant response has been an area of intense research effort over the past 30 years in Europe (Ashmore et al., 2004), largely conducted under the auspices of the United Nations Economic Commission for Europe (UNECE) Long-Range Transboundary Air Pollution (LRTAP) Convention which has established an effects-based approach to air quality management (Bull and Hall, 1998). Over recent years, O_3 characterization indices have moved from a concentration- to a flux-based approach defining O_3 dose as the

ACPD
11, 33583–33650, 2011

effective stomatal O_3 flux or uptake accumulated over a defined growth period (Ashmore et al., 2004; Matyssek et al., 2007). For forest trees, flux-based methodologies have been established and recommended for use in risk assessment by the LRTAP Convention (Karlsson et al., 2004, 2007; Tuovinen et al., 2009; LRTAP Convention, 2010; Mills et al., 2011). Currently, these methodologies use empirically derived flux-response relationships (e.g. Karlsson et al., 2004, 2007) to establish critical levels and to estimate damage in terms of tree biomass loss resulting from stomatal O_3 flux. Therefore, the estimation of O_3 flux is one crucial component necessary to assess O_3 risk to forest trees. The estimation of actual damage requires knowledge of the effective O_3 dose, i.e. the fraction of stomatal O_3 flux that the plant is unable to detoxify without loss of vigour (cf. Musselman et al., 2006; Matyssek et al., 2008). The plants detoxification capacity is known to vary with genotype (Karnosky et al., 1998), species (Karlsson et al., 2007), tree age (Wieser et al., 2002) and diurnal (Schupp and Rennenberg, 1988; García-Plazaola et al., 1999; Peltzer and Polle, 2001; Wieser et al., 1995) and seasonal (Luwe, 1996; García-Plazaola and Becerril, 2001) conditions such that current empirical flux-based dose-response relationships may struggle to incorporate the complexities of the damage response (Musselman et al., 2006).

In this paper we focus on the estimation of the stomatal O_3 flux component to enable an assessment of the potential for O_3 damage to forest trees. The model currently used to estimate O_3 fluxes to representative vegetation types (which include crops and semi-natural vegetation as well as forests tree species) across Europe is the DO_3SE (Deposition of O_3 and Stomatal Exchange) O_3 dry deposition model (Emberson et al., 2001), which is embedded within the EMEP (European Monitoring and Evaluation Programme) photo-chemical model (Simpson et al., 2003a, 2007; Tuovinen et al., 2004). DO_3SE estimates O_3 flux to vegetated surfaces as a function of O_3 concentration, meteorology and plant-specific characteristics (including phenological, physiological and structural characteristics). At the core of this model is the estimate of stomatal conductance (g_{sto}), currently achieved using a multiplicative g_{sto} algorithm based on that originally established by Jarvis (1976) and modified for O_3 deposition

ACPD
11, 33583–33650, 2011

and risk assessment by Emberson et al. (2000a,b, 2001). This model has been parameterised for four evergreen tree species, i.e. Norway spruce (*Picea abies*), Scots pine (*Pinus sylvestris*), Aleppo pine (*Pinus halepensis*) and holm oak (*Quercus ilex*), and three deciduous species, i.e. birch (*Betula pendula*), beech (*Fagus sylvatica*) and temperate oak (*Quercus robur* and *Q. pretraea*). For some of these species, climate specific parameterisations have also been established to allow for ecotypic variation in g_{sto} response to climatic variables (LRTAP Convention, 2010). The DO_3SE model and its variations have been extensively evaluated for different forest species, in different countries, under a variety of seasonal conditions (e.g. Tuovinen et al., 2004; Emberson et al., 2007; Nunn et al., 2005). However, one fundamental obstacle to European-wide application of the flux modelling method has been the difficulty associated with estimating soil water status and its influence on g_{sto}.

To date, European application of the DO_3SE model within the EMEP photo-chemical model for O_3 risk assessments has been restricted by the approximation of soil water not limiting g_{sto} and subsequent O_3 flux (e.g. Simpson et al., 2007), except for some sensitivity studies that have investigated the influence of soil water deficit on O_3 flux (e.g. Simpson et al., 2003b; Nunn et al., 2005). This is perhaps not such an issue for agricultural crops receiving irrigation. However, for forest trees this is a serious limitation to the current modelling methods, particularly in the Mediterranean region, where appropriate flux-based O_3 risk assessments might be compromised by the exclusion of the influence of drought on stomatal O_3 flux (Gerosa et al., 2009). There is also evidence that soil water stress can influence detoxification rates of absorbed O_3 (Matyssek et al., 2006, 2007). High soil moisture deficits will also lead to a reduction in O_3 deposition to vegetated surfaces. This can cause a build up of atmospheric O_3 concentrations through the removal of the vegetation O_3 sink (Solberg et al., 2008; Vieno et al., 2010) with consequences for other receptors, such as increased risk to human health. As such, it is imperative to develop and evaluate methods to estimate the influence of soil water status on stomatal O_3 flux.

ACPD
11, 33583–33650, 2011

Here, we describe the continued development of the DO_3SE soil moisture module (Emberson et al., 2007), which now incorporates the Penman-Monteith model of transpiration (Monteith, 1965) to drive water cycling through the soil-plant-atmosphere system along with empirical data describing g_{sto} relationships with pre-dawn leaf water status to estimate the biological control of transpiration. We trial four different methods to estimate this biological control of the transpiration stream which vary from simple methods that relate soil water content (θ) or potentials directly to g_{sto} (denoted as f_{PAW} and f_{SWP} models) to more complex methods that incorporate hydraulic resistance (steady-state, SS) and plant capacitance (non-steady-state, NSS) to water flow through the plant system.

Evaluation of these new methods incorporated into the DO_3SE model is performed against observed data collected for a number of different tree species (boreal, temperate and Mediterranean species of deciduous, coniferous and broadleaf evergreen forest types). These datasets provide seasonal observations of key parameters that are selected to indicate the level of soil drought and influence on g_{sto} occurring at each site. The soil moisture module is assessed with the aim of providing an indication as to whether this model is "fit for purpose" to estimate, at least in relative terms, the influence that soil moisture deficit may have in regulating stomatal O_3 flux and hence O_3 deposition across Europe. A sensitivity analysis is also performed to establish which aspects of the model (e.g. root depth, maximum g_{sto}, leaf area index (LAI), soil texture) are most important as drivers of soil water status to target future parameterisation efforts as well as to understand the reliability with which the model can be applied to different locations and conditions.

ACPD
11, 33583–33650, 2011

2 Methods

2.1 DO_3 SE model

DO_3SE is a soil-vegetation-atmosphere-transport (SVAT) model that has been specifically designed to estimate O_3 deposition to European vegetation (Emberson et al., 2001). It is unique in relation to other SVAT models since it has been designed to be embedded within a complex regional scale photo-oxidant model developed by EMEP (Simpson et al., 2003a, 2007) to inform European effects-based air pollution emission reduction policy (Sliggers and Kakebeeke, 2004). This means that the modelling of gas transfer between the atmosphere and biosphere needs to be simple enough to ensure reasonable model run times, yet complex enough to incorporate the key drivers of O_3 flux at the European scale. The application of the model across such a large spatial region also means that the complexity of the model has to be balanced against the availability of spatial data characterising the important physical and environmental conditions that will influence O_3 deposition across Europe (e.g. land cover, species distribution, soil type, root depth and meteorological information).

To calculate total O_3 deposition DO_3SE uses a standard resistance scheme to estimate the transfer of O_3 from an atmospheric reference height (i.e. the lowest grid level of the EMEP model) to the sites of O_3 deposition at the vegetated surface. Aerodynamic (R_a), quasi-laminar boundary layer (R_b) and surface (R_{sur}) resistances to O_3 transfer are considered in the scheme. R_a and R_b are calculated according to standard methods as described in Simpson et al. (2003a). R_{sur} is calculated as a function of stomatal (r_{sto}) and non-stomatal canopy resistances, the latter including external plant surface (r_{ext}), aerodynamic within-canopy (R_{inc}) and ground surface/soil resistances (R_{gs}) for which empirical methods and constants are employed based on published literature; see Simpson et al. (2003a) and Simpson and Emberson (2006) for further details. Stomatal and external resistances to O_3 uptake are defined per leaf/needle area (denoted by a lower case r) and for R_{sur} scaled according to LAI and surface area

ACPD
11, 33583–33650, 2011

index (SAI), respectively.

$$R_{sur} = \frac{1}{\frac{LAI}{r_{sto}} + \frac{SAI}{r_{ext}} + \frac{1}{R_{inc}+R_{gs}}} \quad (1)$$

The LAI scaling employs a canopy light extinction model to estimate sunlit and shaded canopy fractions and hence scales stomatal resistance as a function of radiative penetration into the canopy (Norman, 1982).

The DO_3SE model employs a multiplicative algorithm, based on that first developed by Jarvis (1976), modified for O_3 flux estimates (Emberson et al., 2000a; 2000b; 2001; 2007) to estimate leaf/needle stomatal conductance (g_{sto}, the inverse of r_{sto}) as:

$$g_{sto} = g_{max} f_{phen} f_{light}{}^{max} \{f_{min}, f_T f_D f_{SW}\} \quad (2)$$

where the species-specific maximum g_{sto} (g_{max}) is modified by functions (scaled from 0 to 1) to account for g_{sto} variation with leaf/needle age over the course of the growing season (f_{phen}) and the functions f_{light}, f_T, f_D and f_{SW} relating g_{sto} to irradiance, temperature, vapour pressure deficit and soil water, respectively. f_{SW} can either be related to soil water potentials (f_{SWP}) or plant available soil water expressed in volumetric terms (f_{PAW}). f_{min} is the minimum daylight g_{sto} under field conditions, expressed as a fraction of g_{max}.

This stomatal component of the DO_3SE model is the primary determinant of the absorbed O_3 dose; the plants internal O_3 detoxification capacity determines the fraction of this dose that is effective in causing plant damage. As such, this leaf-level stomatal flux module forms the basis of empirical flux-based algorithms recommended for use by the UNECE LRTAP to assess European-wide risk of O_3 damage (LRTAP Convention, 2010).

The use of this standard SVAT modelling scheme provides the opportunity to also model water vapour exchange since this follows very similar atmosphere-biosphere exchange pathways as those for O_3 (Fig. 1). This approach also allows for the estimation

ACPD
11, 33583–33650, 2011

of O_3 flux and water vapour transfer to be performed in an internally consistent manner. All symbols and abbreviations used within the DO_3SE model are presented in Table 1.

2.2 Soil water balance

The DO_3SE soil water status module is developed based on the Penman-Monteith model of evapotranspiration, with consideration of the forest canopy and underlying soil (Monteith, 1965; Shuttleworth and Wallace, 1985). As such, soil water loss is driven by evaporative demand limited by a series of soil-plant-atmosphere resistances to water loss which define the variation in water potential (Ψ) across the plant continuum. A simple mass balance calculation is used to estimate the soil water balance over a finite depth of soil determined by a species-specific maximum root depth (d_r) as a function of incoming precipitation and outgoing total evapotranspiration (E_{at}) estimated from plant transpiration (E_t) as well as soil and intercepted canopy evaporation (E_s and E_i, respectively).

Hourly E_t, E_s and E_i are calculated using the Penman-Monteith model (Monteith, 1965). These hourly values are then summed to provide estimates of the water vapour flux on a daily time-step. The estimates use only those resistances to mass transfer that occur between the top of the evaporative surface and the measurement height of vapour pressure deficit (D). We assume that D is provided at the external margin of the canopy boundary layer, consistent with assumptions of constant near-surface D profiles in the EMEP model, with $R_a = 0$. The following formulation describes the Penman-Monteith model for E_t:

$$E_t = \frac{\Delta(\Phi_n - G) + \rho_a c_p(\frac{D}{R_{bH_2O}})}{\lambda\{\Delta + \gamma(1 + \frac{R_{stoH_2O}}{R_{bH_2O}})\}} \quad (3)$$

where Δ is the slope of the relationship between the saturation vapour pressure and temperature, Φ_n is the net radiation above the canopy, G is the soil heat flux, ρ_a is

ACPD
11, 33583–33650, 2011

the air density, c_p is the specific heat of air, R_{bH_2O} is the boundary layer resistance to water vapour exchange, R_{stoH_2O} is the stomatal canopy resistance to transfer of water vapour, γ is the psychrometric constant, and λ is the latent heat of vaporization.

When the soil water is not limiting g_{sto}, the soil will lose moisture through evaporation from the soil surface (E_s) at a rate defined by the Penman-Monteith equation for evaporation modified to include the resistances from the soil surface to the atmosphere:

$$E_s = \frac{\Delta(\Phi_{ns} - G) + \rho_a c_p \left(\frac{D}{R_{inc}+R_{bH_2O}}\right)}{\lambda\{\Delta + \gamma(1 + \frac{R_{soil}}{R_{inc}+R_{bH_2O}})\}} \quad (4)$$

where the soil resistance term to water vapour flow (R_{soil}) is constant at 100 s m^{-1} (Wallace, 1995) and Φ_{ns} is the net radiation available at the soil surface estimated by

$$\Phi_{ns} = \exp(-K_a LAI)\Phi_n \quad (5)$$

where K_a is the coefficient for attenuation of available energy and is set to 0.5 for consistency with the DO$_3$SE module estimates of canopy radiation penetration based on an assumed spherical leaf inclination distribution (Emberson et al., 2000b). When soil water is limiting g_{sto}, such that the upper soil layers are likely to have dried through evaporative water loss, the soil evaporation is assumed to be negligible and hence the term E_s is set to 0.

The total loss of soil water through E_{at} is calculated using the method of Shuttleworth and Wallace (1985) modified to incorporate resistance terms calculated with DO$_3$SE:

$$E_{at} = C_c\, E_t + C_s\, E_s \quad (6)$$

where C_c and C_s are the coefficients of transpiration and evaporation fraction of E_{at} estimated according to

$$C_c = [1 + \frac{ZX}{Y(Z+X)}]^{-1} \quad (7)$$

ACPD
11, 33583–33650, 2011

$$C_s = [1 + \frac{YX}{Z(Y+X)}]^{-1} \quad (8)$$

and

$$X = (\Delta + \gamma)(R_{bH_2O}) \quad (9)$$

$$Y = (\Delta + \gamma)R_{inc} + \gamma R_{soil} \quad (10)$$

$$Z = \gamma\ R_{stoH_2O} \quad (11)$$

Daily recharge of soil water is calculated according to total precipitation (P_{total}) allowing for a fraction lost through interception by the canopy and subsequent evaporation (E_i) so that P_{input} is the fraction of P_{total} that results in soil recharge:

$$P_{input} = (P_{total} - S_c) + (S_c - \min\{E_i, S_c\}) \quad (12)$$

where S_c is the external storage capacity of the canopy that determines the amount of intercepted water. S_c (in m) is defined as 0.0001 LAI using the methodology of Sellers et al. (1996) developed for a range of land cover types including broadleaf and needle leaf trees. E_i is estimated using the Penman equation for evaporation from a wet surface (Monteith, 1965):

$$E_i \frac{\Delta(\Phi_n - G) + \rho_a c_p \left(\frac{D}{R_{bH_2O}}\right)}{\lambda(\Delta + \gamma)} \quad (13)$$

Any water remaining on the canopy at the end of the day is assumed to enter the soil system. At the start of the year, when soil water calculations are initialized, θ (volumetric soil water content) is assumed to be equal to field capacity (FC). The volumetric FC defines the relative amount of water held by capillarity against drainage by gravity and is dependent on soil texture (Foth, 1984). At volumetric FC, the soil water storage (S_n) term, expressed over the entire root depth (S_n/d_r), is assumed to be at a maximum.

ACPD
11, 33583–33650, 2011

Daily estimations of S_n are made according to the mass balance formulation based on those used by Mintz and Walker (1993) where the S_n changes on a daily time step according to

$$S_n = S_{n-1} + P_{\text{input}} - E_{\text{at}} \quad (14)$$

where S_{n-1} is the soil water storage of the previous day, E_{at} is the total water loss to evapotranspiration and P_{input} is water gained via precipitation; any excess P_{input} is assumed to be lost to run-off or percolation from the rooting zone.

Assuming a homogenous root distribution throughout the rooting zone, the physiologically relevant soil water potential (Ψ_{soil}) can be estimated from θ using standard soil water characterisation curves as defined by Campbell (1985).

$$\Psi_{\text{soil}} = \Psi_{\text{e}}\left(\frac{\theta_{\text{sat}}}{\theta}\right)^{b} \quad (15)$$

where Ψ_{e} is the soil water potential at air entry, θ_{sat} is the volumetric soil water content at saturation, and b is an empirical parameter. Where local data are available describing the water holding properties of the soil, site-specific soil water release curves have been constructed and used in the modelling analysis (Table 2). Where no data are available, an estimate is made of the soil texture class on consultation with the holder of the site data and the most appropriate soil water release curve from sandy loam, silt loam, loam or clay loam is used; these curves were established based on parameters given in Tuzet et al. (2003) (Table 3).

2.3 Stomatal conductance (g_{sto})

A number of different methods were assessed to infer g_{sto} from soil water status and hence determine the limiting influence on water transfer from the soil through the tree to the atmosphere. These methods were: (i) f_{PAW}; (ii) f_{SWP}; (iii) steady-state (SS), and (iv) non-steady-state (NSS) and are described in turn below. With the exception of

ACPD
11, 33583–33650, 2011

the f_{PAW} method, all require an estimate of f_{SWP} which is derived from published data describing the relationship between g_{sto} and pre-dawn leaf water potential ($\Psi_{leaf,pd}$). Here we assume that $\Psi_{leaf,pd}$ is equivalent to Ψ_{soil}, a common assumption within soil-plant water balance calculations albeit one that becomes less robust in rapidly drying soils (Slatyer, 1967). This relationship has been defined by fitting a power regression equation to observations of $\Psi_{leaf,pd}$ and relative maximum stomatal conductance (g_{max}) (Fig. 2). These observations were collated from published data for boreal/temperate forest trees represented by beech, temperate oak, Scots pine, Norway spruce and for Mediterranean evergreen forest trees represented by holm oak. Since the data indicate variable tolerance to $\Psi_{leaf,pd}$ between boreal/temperate and Mediterranean forest tree species, we have defined different f_{SWP} relationships for these two forest types as

$$f_{SWP} = \min\{1, \max\{f_{min}, 0.355(-\Psi_{leaf,pd})^{-0.706}\}\} \quad (16)$$

for boreal/temperate forest trees and

$$f_{SWP} = \min\{1, \max\{f_{min}, 0.619(-\Psi_{leaf,pd})^{-1.024}\}\} \quad (17)$$

for Mediterranean forest trees. It is assumed that g_{sto} is increasingly limited until f_{min} is reached, but that past a $\Psi_{leaf,pd}$ of −4 MPa (Ψ_{min}) no more water can be extracted from the soil by the plant. These f_{SWP} curves are soil texture independent and correspond to an approximately linear decrease in relative g_{sto} once volumetric plant available water (PAW) falls below 25 % in boreal/temperate trees and 12 % in the Mediterranean trees, assuming a silt loam textured soil.

f_{SWP}: in this approach g_{sto} is assumed to be limited directly by Ψ_{soil} according to the forest type specific f_{SWP} relationship (cf. Emberson et al., 2007). This is calculated on a daily time-step so that the soil water mass balance calculated for a given day is used to estimate Ψ_{soil} for the following day.

f_{PAW}: in this approach g_{sto} is assumed to be limited by PAW expressed as a function of θ over the root depth, where PAW = FC–PAW_{min}. PAW_{min} is the equivalent soil texture-dependant θ at Ψ_{min}; a linear relationship with a threshold of PAW = 50 % is

ACPD
11, 33583–33650, 2011

used to estimate the effect of PAW on g_{sto} based on empirical data published by Domec et al. (2009). The θ at FC and PAW_{min} are estimated according to the relevant soil water release curves for the specific site conditions. The influence of PAW on g_{sto} is calculated on a daily time-step so that the soil water mass balance calculated for a given day is used to estimate θ and PAW for the following day.

SS: The SS model controls water flux on an hourly time-step using an estimation of leaf water potential (Ψ_{leaf}) based on the daily Ψ_{soil} and plant transpiration of the previous hour. The influence of Ψ_{leaf} on hourly g_{sto} is estimated using the forest type specific f_{SWP} relationship for $\Psi_{leaf,\,pd}$. Ψ_{leaf} is calculated using the standard steady-state formulation (e.g. Van den Honert, 1948; Landsberg et al., 1976; Larcher, 2003):

$$E_t = \frac{\Psi_{soil} - \Psi_{leaf}}{R_{sr} + R_p} \tag{18}$$

In this scheme resistances to water transfer from soil to leaf are represented by the soil-root resistance (R_{sr}) and plant hydraulic resistance (R_p) which are both assumed to be constant; xylem resistance due to drought induced embolism is not included in this scheme. R_p (MPa h mm^{-1}) is parameterised according to Mencuccini and Grace (1996) for boreal/temperate forests and Lhomme et al. (2001) for Mediterranean forests as described in Table 1. The resistance to water flow from the soil to the roots (R_{sr}) is calculated after Lynn and Carlson (1990) and Rambal (1993) according to

$$R_{sr} = \frac{k_1}{d_r K_s} \tag{19}$$

where k_1 is a constant related to root density, with a value of 3.5×10^{-12} when R_{sr} is expressed in MPa (mm h^{-1})$^{-1}$, d_r is given in m and K_s (m s^{-1}) is the soil hydraulic conductivity estimated according to standard principles (e.g. Jones, 1992; Lhomme et al., 2001) by

$$K_s = K_{sat}\left(\frac{\Psi_{sat}}{\Psi_{soil}}\right)^{\frac{3}{b+2}} \tag{20}$$

ACPD
11, 33583–33650, 2011

where K_{sat} is the saturated soil hydraulic conductivity and Ψ_{sat} is Ψ_{soil} at field saturation. To ensure internal consistency, K_{sat}, b and Ψ_{sat} are also defined using the soil texture specific parameters of Tuzet et al. (2003) as described in Table 3 or local data where available.

E_t and Ψ_{soil} are estimated in DO_3SE on an hourly time-step so that Ψ_{leaf} can be calculated by re-arranging Eq. (18).

NSS: The NSS approach is similar to the SS approach in that g_{sto} is controlled by Ψ_{leaf}, which is estimated by Ψ_{soil} and the evaporative demand of the tree. Water status is linked to g_{sto} in the same way using f_{SWP}. However, the NSS model, rather than assuming instant equilibration in Ψ between soil and plant as is the case for the SS model, incorporates a lag in stomatal response by estimating a plant capacitance term, essentially allowing for variable water storage within the plant. This lag may be important in the estimation of O_3 deposition to plant tissue given the potential for O_3 concentrations to vary significantly over the course of the day.

This NSS approach is based on that of Lhomme et al. (2001) and includes both the plant capacitance as well as hydraulic resistance terms, allowing for diurnal flux of water to and from the plants water storage reservoir. Plant flux is represented as

$$E_t = \left(\frac{\Psi_{soil} - \Psi_{leaf}}{R_{sr} + R_p}\right) + \left(\frac{\Psi_r - \Psi_{leaf}}{R_c}\right) \quad (21)$$

where the soil-plant water flux is controlled as before and the storage-destorage flux within the plant is controlled by the reservoir potential (Ψ_r) and resistance to such flux (R_c). Changes in Ψ_r over time are determined by the plant capacitance (C) expressed in mm MPa^{-1} (Lhomme et al., 2001). C, R_c and R_p are all entered as empirically derived constants (Table 1).

We assume that Ψ_{leaf} equilibrates with Ψ_{soil} overnight and hence at the start of each day the equation is initialised at $t = 0$ as $\Psi_{leaf} = \Psi_{soil}$; however, we acknowledge that in practice such equilibration is not always achieved (Sellin, 1999). The physiologically

ACPD
11, 33583–33650, 2011

relevant $\Psi_{leaf,pd}$ is calculated for each day using the bulk change in soil water over the d_r based on E_t. Changes in Ψ_{leaf} are calculated for each hour as

$$\Delta\Psi_{leaf} = \left[\frac{\Psi_{soil} - \Psi_{leaf}(t) - (R_{sr}+R_p)E_t(t)}{C(R_{sr}+R_p+R_c)}\right]\Delta t - \left[\frac{(R_{sr}+R_p)R_c}{R_{sr}+R_p+R_c}\right]\Delta E_t \quad (22)$$

$$\Psi_{leaf}(t) = \Psi_{leaf}(t-1) + \Delta\Psi_{leaf} \quad (23)$$

where $\Psi_{leaf}(t-1)$ is the Ψ_{leaf} of the previous hour. As for the SS model the influence of Ψ_{leaf} on g_{sto} is made according to the forest type specific f_{SWP} relationships.

2.4 Phenology

For the boreal/temperate deciduous tree species, growing seasons were defined according to empirical relationships between latitude and leaf flush and fall which have been shown to be consistent with remotely sensed data collected for Europe (LRTAP Convention, 2010). The start of the growing season (SGS) is defined as the initiation of plant physiological activity or leaf flush and is assumed to occur at year day 105 at 50° N and change by 1.5 days per degree latitude earlier moving south, and later moving north. The end of the growing season (EGS) is defined as the onset of dormancy and is assumed to occur at year day 297 at 50° N and change by 2 days per degree latitude earlier moving north, and later moving south. The effect of elevation on phenology is incorporated by assuming a later SGS and earlier EGS by 10 days for every 1000 m above sea level. For Mediterranean evergreen trees, a year round growth period is assumed. Estimations of LAI are based on observations of the variation of LAI over the course of the growth period and defined according to species-specific minimum and maximum LAI values. This ensures that the variation in phenology experienced across Europe is used to define species-specific annual profiles of LAI; further details are provided in LRTAP Convention (2010). For forest trees SAI is equal to LAI + 1 to account for the trunk and branches of the tree (LRTAP Convention, 2010).

ACPD
11, 33583–33650, 2011

3 DO_3SE model application and evaluation

Datasets to evaluate the DO_3SE model were selected according to the following criteria: (i) they represent forest species for which it is possible to define the necessary DO_3SE model parameterisation; (ii) they represent a range of different forest species functional types (e.g. conifers, deciduous and broadleaf evergreen species) and (iii) they are derived from locations covering the broad climatic regions of Europe (e.g. boreal, temperate and Mediterranean), either within Europe or from analogous sites in North America.

Ten forest datasets were found that met these criteria (site details are provided in Table 4) and were available for evaluation modelling. These datasets were collected in Sweden (Asa, Norunda), Switzerland (Davos), Germany (Forellenbach, Hortenkopf, Kranzberger Forst) and Spain (Miraflores de la Sierra, Prades) and the USA (Rhinelander, WI; Strawberry Peak/Crestline, CA). These North American datasets are included in this European analysis since it was considered that the forest types and prevailing climatic conditions were similar to those found in northern Europe (Rhinelander) and the Mediterranean (Strawberry Peak/Crestline).

To be suitable for DO_3SE model evaluation, each dataset was required to have a complete (or near complete) complement of hourly meteorological data, ideally for a whole year or at least covering the period during which the trees were physiologically active. The required meteorological variables were: temperature (T), precipitation (P), wind speed (u), vapour pressure deficit (D), net radiation at the canopy (Φ_n) and fractions of direct (I_{dir}) and diffuse (I_{diff}) sunlight. The u data were height-corrected to represent u at canopy height. The Kranzberger Forst dataset included meteorological data from a nearby weather station (Waldklimastation Freising, S. Raspe, personal communication, 2010). The Crestline/Strawberry Peak dataset comprised soil water values from two sites and meteorological values from a weather station at a third site; soil water data from both sites are represented separately (Grulke, 1999). The meteorological data for Miraflores were recorded at the nearest weather station, all other

ACPD
11, 33583–33650, 2011

datasets collected meteorological and soil water data at the same site location.

Some variables (T, P, u) were recorded at all sites and were suitable to be used directly as model input. For most sites, D was not recorded but calculated from relative humidity and temperature using standard methods as described in Jones (1992).

Φ_n, required for estimating E_{at}, was not measured at any site and hence was estimated from total radiation (Φ) or photosynthetically active radiation (PAR) using a standard method (FAO, 1998). Similarly, I_{dir} and I_{diff}, required to estimate the *PAR* available to sunlit and shaded leaves, were derived from Φ based on estimated atmospheric transmissivity using the method described by Jones (1992). Soil heat flux G (Eqs. 3, 4 and 9) was calculated as 10 % of Φ_n. For sites where only PAR was recorded (i.e. Davos, Hortenkopf), this was converted to Φ before the above steps were performed.

Where meteorological data were missing for periods of a few hours, data gaps were filled using a linear interpolation between adjacent data points. For the Miraflores 2005 dataset, 14 days worth of data were not recorded (14–31 July). In this case, gap-filling of the dataset was achieved using hourly averages representing the relevant diurnal time for the periods 3–13 July and 1–10 August; it was assumed that no rain fell during this period.

For evaluation purposes, the datasets were also required to comprise frequent seasonal observations of variables describing soil water status. Suitable parameters included: Ψ_{soil}, θ, all recorded at specified depths, and PAW and $\Psi_{leaf,\ pd}$, which were assumed to represent the soil water status of the entire root depth. For the former, the model parameter d_r was set equivalent to the soil depth represented by the measurements; for the latter, d_r was defined either by local data or according to DO_3SE default values provided in Table 2. Field data on these soil water status variables were collected in a range of units and comparisons are presented in original units to minimise errors. Ideally, since the objective of the model is to estimate g_{sto} for the calculation of stomatal O_3 flux, observations of g_{sto}, or relevant variables, would also be available for comparison. However, such measurements were only available for a limited number of sites. E_t data comparisons are provided where possible to give an indication of the

ACPD
11, 33583–33650, 2011

biological control of soil water flux from the system, though it is recognised that such comparisons are not ideal for inferring the influence of soil moisture on stomatal O_3 flux since *Et* is in part driven by the atmospheric water status whilst stomatal O_3 flux is partly dependent upon the ambient O_3 concentration. For those sites where E_t or g_{sto} data do exist, totals or daily maxima respectively were compared to equivalently presented modelled values.

In the absence of local data describing soil texture, the model runs were performed with the most appropriate of the four soil textures (Table 3), defined according to site-specific information where this was available or by calibrating modelled with observed FC under conditions when it would be expected that the soil was fully recharged and precipitation moderate.

Table 2 describes the model parameterisations for each site used in this evaluation. Where possible, local parameterisations of g_{max} and LAI were used; where these were unavailable, default DO_3SE model parameterisations were used based upon values given in LRTAP Convention (2010) which provide representative values for tree species in several European regions (Northern, Atlantic Central, Continental Central and Mediterranean).

One set of model runs was carried out for all sites and years for which data were available, each of the four modelling methods were applied. Figures 3 to 11 and S1 to S15 (Supplement) show the results of comparisons between the modelled and measured soil water variables in relation to local precipitation data; E_t and g_{sto} are also shown for those sites where comparable data were available.

Statistical analyses of the performance of all four models were carried out by comparing observed and modelled values of soil water (expressed as θ, Ψ_{soil} or PAW) using a set of statistical tests consisting of the coefficient of determination (R^2), mean bias (MB), root mean square error (RMSE) and Willmott's index of agreement (IA); for definitions see Willmott (1982).

ACPD
11, 33583–33650, 2011

3.1 Sensitivity analysis

A sensitivity analysis was performed for those parameters (g_{max}, LAI, d_r and soil texture) which were considered particularly important in determining soil water status, g_{sto} and E_t. Each parameter was altered by +/−25 %, which kept the changes in parameters within the bounds of realistic values (Breuer et al., 2003) and also allowed an assessment of the relative importance of each parameter to the same magnitude of change. The exception to this was the assessment of the effect of soil texture, which was performed by comparing sandy loam (coarse) and clay loam (fine) parameters, representing extreme soil texture characteristics.

The accumulated Phytotoxic Ozone Dose (i.e. the accumulated stomatal flux) of O_3 above a flux threshold of 1 nmol m^{-2} s^{-1} per leaf area for forest trees (POD_1; LRTAP Convention, 2010) was used to determine the sensitivity of the different parameters to O_3 flux since it represents a model output parameter that integrates the soil water modelling to a single seasonal ozone flux variable. The sensitivity analysis was carried out for the Norunda site for which data were available for 1999. This dataset was chosen since it represents a year with substantial water stress at a well observed site (both in terms of soil water status and E_t variables).

4 Results

Figures 3 to 11 compare modelled with measured soil water variables. Depending on data availability, variables related to soil water influence on leaf conductance (i.e. E_t and g_{sto}) are also shown. For all soil water related results (i.e. θ, Ψ_{soil} or PAW), predictions are given for all four models. For f_{SWP}, E_t or g_{sto} predictions, only results from the best performing model for that site (according to the performance statistics provided in Table 5) are shown. Figures describing results for Asa in 2000 and Davos in 2004 are not shown in the paper due to the fact that these sites experienced no drought in these years. However, together with more detailed results from other sites,

ACPD
11, 33583–33650, 2011

these findings are shown in the Supplement (Figs. S1 to S16).

One of the most important aspects of the model to evaluate is the capability of predicting the length and severity of drought periods, and the influence of such soil drought on canopy g_{sto} since this will determine stomatal O_3 flux. As such, this is the aspect crucial to the DO_3SE model since it will determine the potential risk posed by O_3. Thus, when comparing modelled with observed soil water conditions, it is useful to consider the length of soil drying periods that fall below the threshold for the onset of stomatal closure since this represents the point at which g_{sto} is restricted by reduced soil water availability and therefore indicates periods when the DO_3SE model will assume soil water limited stomatal O_3 flux. The effect of soil drought on canopy conductance can specifically be investigated for the Norunda, Rhinelander and Kranzberger Forst sites which provide details of observations of soil water variables as well as canopy conductance variables (either E_t or g_{sto}). Results comparing modelled and measured variables in relation to P events are shown for each of these sites in Figs. 3 to 5.

The coniferous forest at the Swedish site Norunda experienced serious drought conditions during the summer of 1999 (Figs. 3, S10 and S11). A measured minimum θ of approximately 0.05 $m^3\,m^{-3}$ was fairly accurately predicted by the f_{SWP}, f_{PAW} and NSS approach. The θ falls below the minimum for the onset of stomatal closure for approximately 25 days from day of year 190, resulting in a strongly reduced E_t and hence stomatal O_3 flux (Figs. 3 and S10). The seasonal course of the increasing drought can also be seen in the decreasing f_{SWP} values from day 150 onwards (Fig. 3). Single rainfall events ease the drought effects during the summer resulting in a temporary increase in E_t, but the soil water recharges only after heavy rainfall in late September.

The North American Rhinelander site comprised both pure aspen as well as mixed aspen-birch forest stands; parameterisations for both forest types were defined in terms of LAI and g_{max} (Table 2). The model runs for both parameterisations revealed no significant differences of soil water effects on g_{sto} in relative or absolute terms; hence Fig. 4 (and Figs. S13 and S14) only show the results for the mixed aspen-birch forest. The site remained fairly wet during the beginning of the 2006 growing season with

ACPD
11, 33583–33650, 2011

no obvious effect on f_{SWP} and hence E_t. However, soil water conditions in the first 65 cm of the soil became considerably drier in June, resulting in a sharp drop in θ, f_{SWP} and, to a lesser extent, E_t (Figs. 4, S13 and S14). All four models capture the timing of the drought effect and its extent during the summer well, but underestimate and overestimate θ in spring and autumn respectively. Also, during the earlier part of the drought period the measured maximum E_t is higher than that predicted by the model (Figs. 4 and S13). However, both measured and modelled E_t data show a dip during the driest period at around day 200.

The year 2003 was characterised by a prolonged drought period in Central Europe. This is mirrored by the fairly low P levels at Kranzberg. Measured data of θ show a drop from 0.38 to approximately 0.25 $m^3\,m^{-3}$ during the drought period, which is best mimicked by the NSS model, whereas the f_{SWP} and f_{PAW} models overestimate and the SS model underestimates the drought effect on θ. However, all models capture the period of reduced θ well and the match between observed and modelled θ is satisfactory at the beginning and end of the growing period. Also, all models apart from the SS model showed a distinct drop in f_{SWP} during the drought period in late summer (Figs. 5 and S7). Up until August, modelled and observed g_{sto} tended to match each other, although by September, towards the end of the drought period, observed g_{sto} showed a clear recovery (Fig. 5), which may have been related to precipitation events during this period. Observations showed that such events only moistened the uppermost 5 cm of the soil profile. Since this is the densely rooted litter layer, wetting may have resulted in increased water availability to the plant that would have been under-represented by the soil water balance model which integrates soil moisture within the uppermost 40 cm of the profile. In addition, since all models relate g_{sto} either directly or indirectly to Ψ_{soil}, they were unable to capture the observed increase in g_{sto} (Figs. 5 and S6). Discrete porometry-based measurements conducted in parallel during that period also showed some recovery in g_{sto}, although to a lesser extent than by the approach depicted in Fig. 5 (Löw et al., 2006).

ACPD
11, 33583–33650, 2011

Model runs for Asa, Sweden were carried out for the year 1995 and 2000 (Figs. 6, S1 and S2). While in 2000 soil water conditions were hardly limiting g_{sto} of the Norway spruce stand (Fig. S1), in 1995 a distinct drought period in August lead to a decrease in Ψ_{soil} as depicted both in modelled and measured data (Figs. 6 and S1). The extent of the drought effect is best captured by the f_{PAW} and f_{SWP} models, whereas the SS and NSS models clearly overestimate Ψ_{soil} and predict the soil to remain far wetter. This difference between models is also mirrored by the f_{SWP}: this parameter is strongly reduced during August 1995 only in f_{PAW} and f_{SWP} model predictions.

Similar statements can be made about the Forellenbach results (Figs. 7 and S4), where in the dry year 2003 the PAW steadily decreased to a minimum of approximately 40 mm at the end of August, with an obvious limiting effect on g_{sto} starting in late July: the f_{PAW} and f_{SWP} models clearly outperformed the SS and NSS models.

Figs. 8 and S5 show the year-to-year variation in θ for the central European mixed beech and oak forest at Hortenkopf. Observed and modelled θ confirm the relative wetness of 2000, followed by three years of clear drought effects, with 2003 being the driest year. The f_{PAW} and f_{SWP} models perform well during all years, capturing the periods and extent of drought, expressed as θ, well. The performance of the SS and NSS models are much less satisfactory (Fig. 8). These results are also mirrored by the diurnal course of the f_{SWP} as shown in Fig. S5. Episodic rainfall events in between periods of distinct dryness led to an almost full recharge of soil water at several times during the growing seasons 2001 and 2002, but not in 2003 (f_{PAW} and f_{SWP} models, Fig. S5).

Results of model runs for evergreen oak forest sites with Mediterranean climatic conditions (two Spanish, one Californian site) are shown in Figs. 9 to 11 (and Figs. S8, S9, S12, S13 and S16). These sites are more prone to drought conditions with the figures showing limited θ during the summer time. The sites Miraflores de la Sierra and Prades are of particular value for this study, since they provide multi-year model input and validation data (though the latter is far from continuous), so model runs spanning more than one growing season could be assessed.

ACPD
11, 33583–33650, 2011

At the Miraflores site (Fig. 9), a total recharge of the soil water was experienced during the winter of 2004/2005 due to some heavy rainfall in autumn and winter (Fig. S9). In 2004, only the f_{SWP} model was able to capture the very low Ψ_{soil} at the end of the summer, whereas in 2005 all models predicted the drought-induced low Ψ_{soil} for most of the summer as also observed at the site. These results are also mirrored in the seasonal course of the f_{SWP} as shown in Fig. S9. During both summers, the f_{SWP} dropped to its minimum value of 0.2 using thef_{SWP} model (Fig. S9), leading to a reduction of g_{sto} during drought periods (results presented in Alonso et al., 2008).

In contrast, the Prades holm oak site did not experience a full recharge of soil water during the winters of 2001/2002 and 2002/2003 despite some rainfall during the autumn and winter months (Figs. 10 and S12). However, while the θ clearly shows the missing soil water recharge at the end of 2001 and 2002, this effect actually only affects g_{sto} – expressed as the multi-annual course of f_{SWP} in Fig. S12 – when using the f_{PAW} model, i.e. with all three other models the g_{sto} is for a long time unaffected by drought at the beginning of the years 2002 and 2003. When comparing the few available measured with modelled θ data, it seems that all models slightly underestimate the θ during the winter months, but catch well the θ during the drought period in 2003 (Fig. 10).

The Strawberry Peak/Crestline evergreen oak site experienced severe drought conditions in 1995 (Figs. 11 and S15). The f_{SWP} and f_{PAW} models predict the decline in θ quite well until the end of July, but afterwards overestimate θ; the two other models consistently overestimate the θ at the site as compared to measured data (Fig. 11). Furthermore, the f_{SWP} and f_{PAW} models predict that despite an early decline in θ from April on, only in mid June dramatic effects of drought on f_{SWP} and hence g_{sto} are experienced (for the SS and NSS models, this effect appears even later in the year) (Fig. S15).

When comparing the overall performance of all four models with help of the set of statistical parameters given in Table 5, it is apparent that the f_{SWP} and f_{PAW} models almost always outperform the SS and NSS models, with the SS model showing on average the worst statistical agreement between observed and modelled data as indicated by

ACPD
11, 33583–33650, 2011

low R^2 and IA values on the one hand and comparatively high values of MB and RMSE on the other. The poorer performance of the SS and NSS model is also mirrored by the much smaller number of days when f_{SWP} is predicted to fall below 1 for these two models as compared to the f_{SWP} and f_{PAW} models (Table 6), suggesting a less pronounced effect of dry soil water conditions on g_{sto}. To distinguish between the performance of the f_{SWP} and f_{PAW} models is more difficult, since both models perform well and in a very similar fashion when applied to datasets in which clear drought conditions have been experienced (Table 6).

The results of the sensitivity analysis, performed for the Norunda site, are shown in Table 7. They reveal that a variation in the soil texture and g_{max} parameters lead to the biggest change in POD_1 regardless of the model used, with clay loam as compared to sandy loam and a decreased g_{max} resulting in a smaller change in POD_1 (a reduction of up to 46 %), whereas an increase in g_{max} substantially increases (up to 35 %) POD_1. In comparison, changes in d_r and LAI led to much smaller – and, depending on the model, sometimes contradictory – changes in POD_1. A reduced consistency in model predictions when using the SS and NSS model as compared to the f_{SWP} and f_{PAW} models also manifests itself in a larger variation in the number of days predicted with f_{SWP} less than 1 for the two former models (Table 7), further confirming the results of the statistical analysis that the f_{SWP} and f_{PAW} models are more reliable.

5 Discussion

This study has investigated four different modelling approaches that provide estimates of soil water, expressed as Ψ_{soil} or θ, and its influence on g_{sto} using the DO_3SE model. This approach provides more consistency in estimates of both water vapour and ozone flux between the atmosphere and the plant system. The f_{SWP} and f_{PAW} models use an empirical approach to relate soil water status to g_{sto}. The difference between these two models is the assumed relationship between soil water status and g_{sto}. The f_{SWP} model uses empirical relationships derived from data for temperate/boreal and Mediterranean

ACPD
11, 33583–33650, 2011

species (Fig. 2) describing the connection between $\Psi_{leaf,pd}$ as a surrogate for Ψ_{soil} (Slatyer, 1967) and leaf g_{sto}. The f_{PAW} model represents a more generic approach by relating soil water status, assessed in terms of PAW, to g_{sto}, assuming a limitation on g_{sto} once less than 50 % of PAW is available (consistent with findings published by Domec et al. (2009) for forest tress). By contrast, the SS and NSS models also use the empirical relationships of the f_{SWP} approach (i.e. they relate $\Psi_{leaf,pd}$ to leaf g_{sto}), but in addition allow for hydraulic resistance (SS) and plant capacitance (NSS) to control water flow through the plant system.

Tables 6 and 7 provide summary statistics for the performance of all four models. Considering those sites and years for which soil water deficits occurred (defined as water deficits that resulted in some stomatal limitation for some part of the year as estimated by at least one of the models), the statistics suggest that a ranking of the models with regard to their predictive performance is $f_{PAW} = f_{SWP} >$NSS > SS. The f_{SWP} and f_{PAW} models describe fairly consistently the highest proportion of variance (R^2- and IA-values of up to 0.94 and 0.97 respectively) and show the smallest absolute difference (fairly consistently low RMSE-values) between modelled and observed data.

The models' performances vary from site to site and year to year. In general, the f_{PAW} and f_{SWP} models (and with less frequency the NSS and SS models) capture the seasonal course of the observed soil water conditions and the magnitude of drought reasonably well. However there are some cases, especially at the beginning and the end of the growing season, where a more substantial divergence between observed and modelled data occurs. For instance model predictions for the Rhinelander, Kranzberg and Forellenbach sites struggle to accurately reflect the rate with which the initial soil drying takes place, often estimating earlier and more prolonged periods of reduced soil water than actually occur.

A direct comparison of the f_{PAW}, f_{SWP}, SS and NSS models (Figs. 3 to 11) shows that the two latter models predicted lower E_t and less dry soil water conditions (expressed as θ, Ψ_{soil} or PAW) as compared to observed data for all sites. This resulted in higher transpiration rates (e.g. Figs. S10 and S13). This finding is not surprising, given that

ACPD
11, 33583–33650, 2011

the SS and NSS models introduce additional resistances to water transfer through the soil-plant-atmosphere continuum. These models were developed to account for the lag effect caused by internal plant resistance to water transfer from the soil-root to leaf-atmosphere interfaces. The water supply from the soil will not always meet the demand resulting from the driving force of a drier atmosphere, resulting in a difference between the soil water status and leaf water status. The NSS model predicts slightly drier (and therefore more realistic, as judged by observed data) soil conditions than the SS model, because the former accounts for a plant capacitance term, representing a buffering effect of water storage in trunk and branches, which causes a lag in g_{sto} response.

The application of the SS and NSS models within the DO_3SE modelling scheme needs further consideration and testing since it may be that the resistance to water transport within the plant can substitute for the f_D function which is currently a component in the estimate of g_{sto}. Similar concepts have been explored for forest trees by Uddling et al. (2005) through the development of models that relate the sensitivity of g_{sto} to D to the accumulated time after sunrise with D exceeding a defined threshold, hence indirectly accounting for hydraulic resistance effects. Additionally, a sum D function developed by Pleijel et al. (2007) that is currently used in the DO_3SE model for crop species (i.e. wheat and potato) is intended to account for a similar reduced water supply to the leaf. Under conditions of continuous and high D levels (most likely to occur in the late afternoon of exceptionally hot and dry days), the stomata are prevented from re-opening even if D levels decrease. Again, this limitation of g_{sto} in response to increasing D attempts to mimic severe leaf water loss and the inability of water from the soil to replenish supplies in the leaf. The subsequent reduced loss of water from the system under high D may in part explain the underestimation found in model estimates of soil drying and subsequent limitations to g_{sto}. The capacitance term in the NSS model buffers this hydraulic resistance to water loss so that the plant is able to meet D-driven transpirational demand until the plant water storage is depleted. As such, more water can be lost from this system compared to the SS system, but the inclusion

ACPD
11, 33583–33650, 2011

of the hydraulic resistance term reduces water loss in comparison to the f_{SWP} and f_{PAW} models.

The modelling approaches presented have been used by a number of other studies, with some favouring the f_{SWP} (e.g. Gao et al., 2002; Emberson et al., 2007) and others favouring the f_{PAW} approach (e.g. Gollan et al., 1986; Grünhage and Haenel, 1997; Granier et al., 2000; Van Wijk et al., 2000; Schwalm and Ek, 2004). However, the f_{PAW} model is often favoured since θ is much more commonly measured in ecological studies. Also, the f_{SWP} model requires that the g_{sto} response to soil water stress be defined in terms of Ψ (i.e. Ψ_{max} and Ψ_{min}), which becomes very sensitive to changes in θ as the soil dries; hence, the modelled limitation to g_{sto} may be extremely responsive to small changes in θ that are close to the equivalent Ψ_{min} threshold value.

Other studies that adopted the SS approach of water transfer within plant canopies include Tardieu and Davies (1993), Saliendra et al. (1995), Tardieu and Simonneau (1998) and Anderson et al. (2000), whereas for example Williams et al. (1996), Kumagai (2001) and Lhomme et al. (2001) adopted the NSS approach. The latter all state the importance of the capacitance term and hence favour this approach over the SS approach. Hunt et al. (1991) argue that SS models are sufficient for the prediction of daily totals of water uptake via roots, whereas NSS models are necessary for the assessment of the instantaneous rate of water uptake with regard to diurnal variations in the use of the water storage capacitance and transpiration rate.

A sensitivity analysis was performed to test the models' sensitivity to key model parameters. The analysis focussed on g_{max}, LAI, soil texture and d_r. These four parameters were selected because they were considered particularly important in terms of determining the availability of soil water to the plant (soil texture and d_r) and the rate of water loss from the plant (g_{max} and LAI). From the range of frequently observed values defined for each of these parameters (Table 7), it is clear that for all four models a variation of g_{max} by 25 % leads to the largest change in POD_1, followed by soil texture, d_r and LAI. As expected, an increase in g_{max} (increased g_{sto} and hence higher E_t) and d_r (increase in accessible water and hence enhanced water supply from root

ACPD
11, 33583–33650, 2011

to plant) results in higher POD_1 values, whereas the change from a sandy to clay loam soil texture (less extractable water, hence reduced accessibility to soil water leading to enhanced drought effects) reduces the POD_1. The effect of LAI on POD_1 is comparatively marginal and inconsistent, which suggests that only pronounced changes in LAI (as can be found for deciduous trees as the growing season and thus foliage develops) might significantly affect the partition of the canopy into sunlit and shaded fractions with subsequent effects on the light penetration of the canopy and hence g_{sto}. These findings stress the importance of the accurate parameterisation of these key variables and especially g_{max}, as noted previously for Jarvis-type models (e.g. Büker et al., 2007).

There are a number of assumptions behind the modelling schemes used here, irrespective of the type of approach. One of the key difficulties in modelling soil water status lies in the characterisation of the soil environment, both in terms of the soil texture and subsequent soil water holding properties, but also in relation to the rooting environment, with the density and structure of roots likely to vary by species, with depth and according to the severity and evolution of drought conditions. Dynamic approaches to estimates of root depth have been attempted by other models (e.g. Jansson and Karlberg, 2004) and may be an option for future model development. There is also evidence that hydraulic redistribution of water between different parts of the soil may take place (Warren et al., 2007, Domec et al., 2010). However, given the difficulties in defining maximum root depth under optimum soil water supply, the addition of such dynamic methods may suggest accuracy in the model parameterisation which in reality is extremely hard to achieve.

All methods require knowledge of the soil texture and use soil water release curves to define the characteristics and absolute values of the different texture-related soil water properties. An argument often cited in favour of the f_{PAW} models is that they avoid issues related to soil texture since soil water status is expressed as θ. However, these models still require that FC and Ψ_{min} be defined as absolute values, and these vary by soil texture. Saxton et al. (1986) and Warren et al. (2005) have developed means of estimating soil water releases curves based on sand, silt and clay fractions within the

ACPD
11, 33583–33650, 2011

soil. However, application of these methods at particular sites is still confounded by the fact that such fractions vary both horizontally and with depth over quite short distances (cm to m). In the absence of detailed soil data, the only option is to generalise based on what data are available for a particular site or across a particular geographical region.

There are also aspects of water vapour loss from the canopy that may require further consideration. In the past the DO_3SE model has tended to focus on estimating stomatal O_3 flux and hence g_{sto} at the leaf level, and, for forest trees, a leaf that represents a mature leaf of the upper canopy. As such the model has concentrated on estimating conductance for sun leaves. However, a mature forest canopy will comprise both sun and shade leaf morphologies, and sunlit and shaded fractions. The latter will vary over the course of a day and the former over the course of a growing season, and both by species and prevailing climatic conditions. This can have important implications for canopy water loss since, when considering the entire growing season, upper canopy sun leaves will have significantly higher g_{sto} and hence water loss than lower canopy shade leaves. The DO_3SE model accounts for variable sunlit and shaded leaf fractions through implementation of the canopy light extinction model (Norman, 1982). However, there is currently no allowance made for the existence of different sun and shade leaf morphologies within the canopy. This will lead to an overestimate of water vapour loss and possibly O_3 deposition. Such diurnal and seasonal variations in sun-lit vs. shaded foliage proportions, and hence in whole-tree transpiration, may be available from analysis of xylem sap flow assessments in tree trunks (Granier et al., 2000; Köstner et al., 2008; Matyssek et al., 2009), allowing for model validation.

The evaluations presented have shown the capability of both the f_{SWP} and f_{PAW} approaches used within the DO_3SE model to perform under a range of climatic conditions (from Scandinavia, through central Europe to the Mediterranean, and similar climates found in North America) and for a variety of forest species that are representative of those different climates. An important aspect of the models' performance under Mediterranean-type climates is its ability to deal with a lack of complete soil water recharge during the winter months. The results from Prades (Fig. 10), showing a water

ACPD
11, 33583–33650, 2011

loss over three subsequent years without a full recharge during the winter months, suggest that the model is capable of capturing the magnitude of soil recharge and water loss over relatively long periods of time. For the more northerly temperate and boreal forests, phenology becomes especially important since this determines the time during which the forest trees are actively transpiring. Phenology, here defined as the start and end of the growing season, is calculated according to a latitude model that was derived from remotely sensed (Zhang et al., 2004) and observational data describing the onset and dieback of vegetation and leaf flushes and senescence respectively, as described and used by LRTAP Convention (2010). The importance of phenology can be seen in terms of controlling the onset and decline of transpiration, with the model seeming able to provide good estimates both of E_t as well as θ.

This discussion has mainly focussed on aspects of water loss via the transpiration stream (E_t), since this pathway will also be important for stomatal O_3 flux. However, issues related to water loss from the soil (E_s) and evaporation directly from external plant surfaces (E_i) are also important, at least in determining the soil water balance. Modelling of the terms E_t, E_i an E_s has been consistent through use of the Penman-Monteith approach. Yet, still some assumptions have to be made. For soils we assume a cap on the amount of water lost from this reservoir when soil water is limiting g_{sto}, such that we mimic the effect of faster soil drying in the uppermost soil layers. For future model development it may be desirable to divide the soil into two separate compartments, one that represents these uppermost layers and allows soil water status to be influenced by E_s, and the other from which gravitationally held water can only be lost via the transpiration stream. In the evaluations E_s is also tempered by the continuous presence of some LAI or SAI, which will reduce the radiation to the soil, hence limiting E_s. However, were the model to be suitable for application over bare soil, a new approach to implementing the cap to water loss via E_s would be necessary.

Other limiting factors of the model include the omission of various elements of the hydrological cycle, such as snow water and groundwater storage terms. However, for the purposes of the evaluation performed in this paper, which focussed on the

ACPD
11, 33583–33650, 2011

physiologically active plant growth period (when snow is unlikely to be present) and for site conditions which were not known to be affected by water table depth, the omission of these storage terms will have been unlikely to significantly affect the results. Further model development could investigate incorporation of these terms, though groundwater storage may be difficult to deal with in relation to regional scale applications due to limitations in data availability.

In relation to future model development, it is also useful to consider new techniques for model evaluation. Recently, methods have become available for validating modelled O_3 flux to trees with empirical data, derived from assessing the trunk sap flow as a measure of foliage transpiration (Nunn et al., 2007; Köstner et al., 2008; Matyssek et al., 2008). Sapflow gauges can be positioned in tree crowns to distinguish water flow to various parts of the foliage, thereby allowing assessment of the total stomatal O_3 uptake of the canopy. This approach provides direct estimates of stand-level stomatal O_3 flux (determined using allometric tree-stand up-scaling, and provided O_3 concentration is measured within the canopy boundary; cf. Wieser et al., 2008). As such, non-stomatal stand-level O_3 deposition can also be derived when employing the eddy covariance approach in parallel (Nunn et al., 2010). The difference between the whole-stand O_3 deposition provided by eddy covariance methodology and stomatal O_3 deposition as based on the sap flow approach represents the non-stomatal O_3 deposition. Such methods provide the opportunity to compare both E_t and stomatal O_3 flux using complimentary measurement approaches and therefore could provide a valuable tool in future efforts to evaluate, and further develop, the DO_3SE soil moisture model.

The modelling performed in this study has assumed no direct effect of O_3 on g_{sto}. However, O_3-induced damage to stomatal functioning (Maier-Maercker, 1997; Mills et al., 2009; Wilkinson and Davies, 2009, 2010) might well impact estimates of stomatal O_3 flux. Currently, our understanding of how combinations of stress variables such as increased temperature, drought and O_3 interact to influence E_t and hence water balance, both on a short-term and long-term basis, are too limited to be incorporated into modelling studies with any degree of confidence. However, observational data

ACPD
11, 33583–33650, 2011

collected for a mixed deciduous forest by McLaughlin et al. (2007a) illustrate the need to consider such interactions in future research efforts. They found an increase in water use under warmer climates with higher O_3 levels. These changes in water balance led to reduced growth of the mature forest trees with potential implications for the hydrology of forest watersheds (McLaughlin et al., 2007b). Such interactions and ecosystem scale responses will be important to consider in future experimental and modelling studies investigating O_3 and drought interactions.

6 Conclusions

The present study describes the further development and evaluation of the DO_3SE soil moisture module previously described in Emberson et al. (2007). This module has been improved through incorporation of the Penman-Monteith approach to estimate E_t, thereby incorporating energy balance terms in the estimate of soil water status and subsequent effects on g_{sto} and stomatal O_3 flux. Four different modelling approaches of linking soil water conditions to g_{sto} were investigated within the DO_3SE model framework.

The models (especially the f_{SWP} and f_{PAW} models) work well at the European scale for various tree species being capable of differentiating between "wet" and "dry" years and of estimating the onset of both soil drying and soil water recharge periods with a good degree of accuracy for a range of different climates typical for Europe and North America.

Both the f_{SWP} and f_{PAW} could be recommended for regional scale application. However, given that θ tends to be more readily available for evaluation and that the simple assumption of 50 % PAW as a threshold for soil water effects on g_{sto} is easy to parameterise without losing any obvious predictive ability, we recommend the f_{PAW} approach for regional scale application. That said, the more physiologically relevant aspects of the f_{SWP} approach might make this method more suitable for application on a site-specific basis, especially where plant physiological data have been collected which

ACPD
11, 33583–33650, 2011

could be used for more detailed assessment and further development of this modelling approach. Hence, we recommend that the selection of either of these modelling approaches be based upon the aims of any study and the available data.

Future model developments should focus on further evaluating the various soil moisture modelling approaches, using both sap flow and eddy covariance techniques, as well as θ data which is starting to be made available from widespread, routine monitoring networks across Europe (e.g. FUTMON, www.futmon.org). This additional information should also allow optimisation of the parameterisation of the DO_3SE soil moisture module.

In conclusion, this work represents an important step forward in being able to estimate stomatal O_3 flux for risk assessment through the incorporation of a robust method to incorporate the influence of soil water stress on the absorbed O_3 dose of forest trees.

Supplementary material related to this article is available online at: http://www.atmos-chem-phys-discuss.net/11/33583/2011/acpd-11-33583-2011-supplement.pdf.

Acknowledgements. We acknowledge the UK Department of Food and Rural Affairs (Defra) under contract AQ 601 who provided support for this research, as well as funding from the EU Nitro-Europe project (www.nitroeurope.eu) and EMEP under UNECE. We also acknowledge the data contribution by Burkhard Beudert (National Park Bayerischer Wald), Stephan Raspe (Bayerische Landesanstalt für Wald und Forstwirtschaft), Joachim Block and Hans-Werner Schröck (Forschungsanstalt für Waldökologie und Forstwirtschaft, Trippstadt), the insightful contributions to this manuscript provided by Roman Zweifel and Dolores Asensio, and Freya Forrest for help in performing some of the DO_3SE modelling. R. Alonso would like to thank for the financial support from the Spanish projects Consolider Montes CSD2008-00040, CGL2009-13188-C03-02 and CAM-Agrisost.

ACPD
11, 33583–33650, 2011

References

Alonso, R., Elvira, S., Sanz, M. J., Gerosa, G., Emberson, L. D., Bermejo, V., and Gimeno, B. S.: Sensitivity analysis of a parameterization of the stomatal component of the DO_3SE model for *Quercus ilex* to estimate ozone fluxes, Environ. Poll., 155, 473–480, 2008.

Anderson, M. C., Norman, J. M., Meyers, T. P., and Diak, G. R.: An analytical model for estimating canopy transpiration and carbon assimilation fluxes based on canopy light-use efficiencies, Agric. For. Meteor., 101, 265–289, 2000.

Aranda, I., Gil, L., and Pardos, J. A.: Water relations and gas exchange in *Fagus sylvatica* L. and *Quercus petraea* (Mattuschka) Liebl. in a mixed stand at their southern limit of distribution in Europe, Trees, 14, 344–352, 2000.

Ashmore, M., Emberson, L., Karlsson, P. E., and Pleijel, H.: New directions: A new generation of ozone critical levels for the protection of vegetation in Europe, Atmos. Environ., 38, 2213–2214, 2004.

Baumgarten, M., Werner, H., Häberle, K. H., Emberson, L. D., Fabian, P., and Matyssek, R.: Seasonal ozone response of mature beech trees (*Fagus sylvatica*) at high altitude in the Bavarian forest (Germany) in comparison with young beech grown in the field and in phytotrons, Environ. Poll., 109, 431–442, 2000.

Bréda, N., Cochard, H., Dreyer, E., and Granier, A.: Water transfer in a mature oak stand (*Quercus petraea*): seasonal evolution and effect of a severe drought, Can. J. For. Res., 23, 1136–1143, 1993a.

Bréda, N., Cochard, H., Dreyer, E., and Granier, A.: Field comparison of transpiration, stomatal conductance and vulnerability to cavitation of *Quercus petraea* and *Quercus robur* under water stress, Ann. Sci. For., 50, 571–582, 1993b.

Breuer, L., Eckhardt, K., and Frede, H.-G.: Plant parameter values for models in temperate climates, Ecol. Model., 169, 237–293, 2003.

Büker, P., Emberson, L. D., Ashmore, M.R., Cambridge, H. M., Jacobs, C. M. J., Massman, W. J., Müller, J., Nikolov, N., Novak, K., Oksanen, E., Schaub, M., and de la Torre, D.: Comparison of different stomatal conductance algorithms for ozone flux modelling, Environ. Pollut., 146, 726–735, 2007.

Bull, K. R. and Hall, J. R.: Setting international targets for controlling atmospheric emissions of pollutants – now and in the future, Environ. Poll., 102, 581–589, 1998.

Bussotti, F., Cascio, C., Desotgiu, R., Pollastrini, M., Gravano, E., Strasser, R.J., Schaub, M.,

ACPD
11, 33583–33650, 2011

Gerosa, G., and Marzuoli, R.: Ozone stress in woody plants assessed with chlorophyll a fluorescence. A critical reassessment of existing data, Environ. Exp. Bot., 73, 19–30, 2011.
Bytnerowicz, A., Omasa, K., and Paoletti, E.: Integrated effects of air pollution and climate change on forests: A northern hemisphere perspective, Environ. Poll., 147, 438–445, 2007.
Campbell, G. S.: Soil Physics with Basic: Transport Models for Soil-Plant Systems, Elsevier Science Publishers, New York, USA, 150 pp., 1985.
Castell, C., Terradas, J., and Tenhunen, J. D.: Water relations, gas exchange, and growth of resprouts and mature plant shoots of *Arbutus unedo* L. and *Quercus ilex* L., Oecologia, 98, 201–211, 1994.
Dobson, M. C., Taylor, G., and Freer-Smith, P. H.: The control of ozone uptake by *Picea abies* (L.) Karst. and *P. sitchensis* (Bong.) Carr. during drought and interacting effects on shoot water relations, New Phytol., 116, 465–474, 1990.
Domec, J.-C., Noormets, A., King, J. S., Sun, G., McNulty, S. G., Gavazzi, M. J., Boggs, J. L., and Treasure, E. A.: Decoupling the influence of leaf and root hydraulic conductances on stomatal conductance and its sensitivity to vapour pressure deficit as soil dries in a drained loblolly pine plantation, Plant Cell Environ., 32, 980–991, 2009.
Domec, J.-C., King, J. S., Noormets, A., Treasure, E., Gavazzi, M. J., Sun, G., and McNulty, S. G.: Hydraulic redistribution of soil water by roots affects whole-stand evapotranspiration and net ecosystem carbon exchange, New Phytol., 187, 171–183, 2010.
Emberson, L. D., Ashmore, M. R., Cambridge, H. M., Simpson, D., and Tuovinen, J.-P.: Modelling stomatal ozone flux across Europe, Environ. Poll., 109, 403–413, 2000a.
Emberson, L. D., Simpson, D., Tuovinen, J.-P., Ashmore, M. R., and Cambridge, H. M.: Towards a model of ozone deposition and stomatal uptake over Europe, Norwegian Meteorological Institute, Oslo, EMEP MSC-W Note 6/2000, 57 pp., 2000b.
Emberson, L. D., Simpson, D., Tuovinen, J.-P., Ashmore, M. R., and Cambridge, H. M.: Modelling and mapping ozone deposition in Europe, Water Air Soil Poll., 130, 577–582, 2001.
Emberson, L. D., Büker, P., and Ashmore, M. R.: Assessing the risk caused by ground level ozone to European forest trees: A case study in pine, beech and oak across different climate regions, Environ. Poll., 147, 454–466, 2007.
Epron, D. and Dreyer, E.: Stomatal and non stomatal limitation of photosynthesis by leaf water deficits in three oak species: a comparison of gas exchange and chlorophyll a fluorescence data, Ann. Sci. For., 47, 435–450, 1990.
Epron, D. and Dreyer, E.: Photosynthesis of oak leaves under water stress: maintenance of

ACPD
11, 33583–33650, 2011

high photochemical efficiency of photosystem II and occurrence of non-uniform CO_2 assimilation, Tree Physiol., 13, 107–117, 1993a.
Epron, D. and Dreyer, E.: Long-term effects of drought on photosynthesis of adult oak trees (*Quercus petraea* (Matt.) Liebl. and *Quercus robur* L.) in a natural stand, New Phytol., 125, 381–389, 1993b.
FAO: Crop evapotranspiration – Guidelines for computing crop water requirements, ISSN 0254-5284, http://www.fao.org/docrep/X0490E/X0490E00.htm, 1998.
Foth, H. D.: Fundamentals of Soil Science, John Wiley and Sons, New York, USA, 1984.
Gao, Q., Zhao, P., Zeng, X., Cai, X., and Shen, W.: A model of stomatal conductance to quantify the relationship between leaf transpiration, microclimate and soil water stress, Plant Cell Environ., 25, 1373–1381, 2002.
García-Plazaola, J. I. and Becerril, J. M.: Seasonal changes in photosynthetic pigments and antioxidants in beech (*Fagus sylvatica*) in a Mediterranean climate: implications for tree decline diagnosis, Austral. J. Plant Physiol., 28, 225–232, 2001.
García-Plazaola, J. I., Artetxe, U., and Becerril, J. M.: Diurnal changes in antioxidant and carotenoid composition in the Mediterranean sclerophyll tree *Quercus ilex* (L) during winter, Plant Science, 143, 125–133, 1999.
Gerosa, G., Finco, A., Mereu, S., Vitale, M., Manes, F., and Ballarin Denti, A.: Comparison of seasonal variation of ozone exposure and fluxes in a Mediterranean Holm oak forest between the exceptionally dry 2003 and the following year, Environ. Poll., 157, 1737–1744, 2009.
Gollan, T., Passioura, J. B., and Munns, R.: Soil water status affects the stomatal conductance of fully turgid wheat and sunflower leaves, Austral. J. Plant Physiol., 13, 459–464, 1986.
Granier, A., Loustau, D., and Bréda, N.: A generic model of forest canopy conductance dependent on climate, soil water availability and leaf area index, Ann. For. Sci., 57, 755–765, 2000.
Grulke, N. E.: Physiological responses of ponderosa pine to gradients of environmental stressors, In: Oxidant air pollution impacts in the montane forests of Southern California: The San Bernardino Mountain case study, edited by: Miller, P. R. and McBride, J., 126–163, Ecol. Studies, 134, Springer, New York, USA, 1999.
Grünhage, L. and Haenel, H.-D.: PLATIN (PLant ATmosphere INteraction) I: A model of plant-atmosphere interaction for estimating absorbed doses of gaseous air pollutants, Environ. Poll., 98, 37–50, 1997.
Hunt, E. R., Running, S. W., and Federer, C. A.: Extrapolating plant water flow resistances and

ACPD
11, 33583–33650, 2011

capacitances to regional scales, Agric. For. Meteor., 54, 169–195, 1991.
Jansson, P.-E. and Karlberg, L.: COUP model – Coupled heat and mass transfer model for soil-plant-atmosphere system, Dept. of Civil and Environmental Engineering, Royal Institute of Technology, Dept. of Land and Water Resources Engineering, Stockholm, Sweden, Publication, 427, 2004.
Jarvis, P. G.: The interpretation of the variations in leaf water potential and stomatal conductance found in canopies in the field, Philos. Trans. R. Soc. Lond., B 273, 593–610, 1976.
Jones, H. G.: Plants and Microclimate, 2nd ed., Cambridge University Press, Cambridge, 428 pp., 1992.
Karlsson, P. E., Uddling, J., Braun, S., Broadmeadow, M., Elvira, S., Gimeno, B. S., Le Thiec, D., Oksanen, E., Vandermeiren, K., Wilkinson, M., and Emberson, L.: New critical levels for ozone effects on young trees based on AOT40 and cumulative leaf uptake of ozone, Atmos. Environ., 38, 2283–2294, 2004.
Karlsson, P. E., Örlander, G., Langvall, O., Uddling, J., Hjorth, U., Wiklander, K., Areskoug, B., and Grennfelt, P.: Negative impact of ozone on the stem basal area increment of mature Norway spruce in south Sweden, For. Ecol. Manage., 232, 146–151, 2006.
Karlsson, P. E., Braun, S., Broadmeadow, M., Elvira, S., Emberson, L., Gimeno, B. S., Le Thiec, D., Novak, K., Oksanen, E., Schaub, M., Uddling, J., and Wilkinson, M.: Risk assessments for forest trees: The performance of the ozone flux versus the AOT concepts, Environ. Poll., 146, 608–616, 2007.
Karnosky, D. F., Podila, G. K., Gagnon, P., Pechter, P., Akkapeddi, Y., Sheng, D. E., Riemenschneider, M. D., Cole, R. E., Dickson, R. E., and Isebrands, J. G.: Genetic control of responses to interacting tropospheric ozone and CO_2 in *Populus tremuloides*, Chemosphere, 36, 807–812, 1998.
Karnosky, D. F., Werner, H., Holopainen, T., Percy, K., Oksanen, T., Oksanen, E., Heerdt, C., Fabian, P., Nagy, J., Heilman, W., Cox, R., Nelson, N., and Matyssek, R.: Free-air exposure systems to scale up ozone research to mature trees, Plant Biol., 9, 181–190, 2007.
King, J. S., Pregitzer, K. S., Kubiske, M. E., Hendrey, G. R., Giardina, C. P., McDonald, E. P., and Karnosky, D. F.: Tropospheric O_3 compromises net primary production in young stands of trembling aspen, paper birch, and sugar maple in response to elevated atmospheric CO_2, New Phytol., 168, 623–636, 2005.
Köstner, B., Matyssek, R., Heilmeier, H., Clausnitzer, F., Nunn, A. J., and Wieser, G.: Sap flow measurements as a basis for assessing trace-gas exchange of trees, Flora (Jena), 203,

ACPD
11, 33583–33650, 2011

14–33, 2008.
Kumagai, T.: Modelling water transportation and storage in sapwood - model development and validation, Agric. For. Meteorol., 109, 105–115, 2001.
Lagergren, F., Lankreijer, H., Kucera, J., Cienciala, E., Mölder, M., and Lindroth, A.: Thinning effects on pine-spruce forest transpiration in central Sweden, For. Ecol. Manage., 225, 2312–2323, 2008.
Landsberg, J. J., Blanchard, T. W., and Warrit, B.: Studies on the movement of water through apple trees, J. Exp. Bot., 27, 579–596, 1976.
Larcher, W.: Physiological plant ecology, 4th ed., Springer, Berlin, Germany, 513 pp., 2003.
Lhomme, J. P., Rocheteau, A., Ourcival, J. M., and Rambal, S.: Non-steady-state modelling of water transfer in a Mediterranean evergreen canopy, Agric. For. Meteorol., 108, 67–83, 2001.
Löw, M., Herbinger, K., Nunn, A.J., Häberle, K.-H., Leuchner, M., Heerdt, C., Werner, H., Wipfler, P., Pretzsch, H., Tausz, M., and Matyssek, R.: Extraordinary drought of 2003 overrules ozone impact on adult beech trees (*Fagus sylvatica*), Trees, 20, 539–548, 2006.
LRTAP Convention: Manual on Methodologies and Criteria for Modelling and Mapping Critical Loads & Levels and Air Pollution Effects, Risks and Trends. Chapter 3: Mapping Critial Levels for Vegetation, http://icpvegetation.ceh.ac.uk/manuals/mapping_manual.html, 2010.
Luwe, M.: Antioxidants in the apoplast and symplast of beech (*Fagus sylvatica* L.) leaves: seasonal variation and responses to changing ozone concentrations in air, Plant, Cell and Environ., 19, 321–328, 1996.
Lynn, B. H. and Carlson, T. N.: A stomatal resistance model illustrating plant vs. external control of transpiration, Agric. For. Meteorol., 52, 5–43, 1990.
Maier-Maercker, U.: Experiments on the water balance of individual attached twigs of *Picea abies* (L.) Karst. in pure and ozone enriched air, Trees, 11, 229–239, 1997.
Manning, W. J. and von Tiedemann, A.: Climate change: potential effects of increased atmospheric carbondioxide (CO_2), ozone (O_3), and ultraviolet-B (UVB) radiation on plant diseases, Environ. Poll., 219–245, 1995.
Matyssek, R. and Sandermann, H.: Impact of ozone on trees: an ecophysiological perspective, Progress in Botany 64, Springer Verlag Heidelberg, Germany, 349–404, 2003.
Matyssek, R., Le Thiec, D., Löw, M., Dizengremel, P., Nunn, A. J., and Häberle, K.-H.: Interaction between drought stress and O_3 stress in forest trees, Plant Biol. 8, 11–17, 2006.
Matyssek, R., Bytnerowicz, A., Karlsson, P.-E., Paoletti, E., Sanz, M., Schaub, M., and Wieser,

ACPD
11, 33583–33650, 2011

G.: Promoting the O_3 flux concept for European forest trees, Environ. Poll., 146, 587–607, 2007.
Matyssek, R., Sandermann, H., Wieser, G., Booker, F., Cieslik, S., Musselman, R., and Ernst, D.: The challenge of making ozone risk assessment for forest trees more mechanistic, Environ. Poll., 156, 567–582, 2008.
Matyssek, R., Wieser, G., Patzner, K., Blaschke, H., and Häberle, K.-H.: Transpiration of forest trees and stands at different altitude: Consistencies rather than contrasts, Eur. J. For. Res., 128, 579–596, 2009.
Matyssek, R., Karnosky, D. F., Wieser, G., Percy, K., Oksanen, E., Grams, T. E. E., Kubiske, M., Hanke, D., and Pretzsch, H.: Advances in understanding ozone impact on forest trees: Messages from novel phytotron and free-air fumigation studies, Environ. Poll., 158, 1990–2006, 2010a.
Matyssek, R., Wieser, G., Ceulemans, R., Rennenberg, H., Pretzsch, H., Haberer, K., Löw, M., Nunn, J.J., Werner, H., Wipfler, P., Oßwald, W., Nikolova, P., Hanke, D.,Kraigher, H., Tausz, M., Bahnweg, G., Kitao, M., Dieler, J., Sandermann, H., Herbinger, K., Grebenc, T., Blumenröther, M., Deckmyn, G., Grams, T.E.E., Heerdt, C., Leuchner, M., Fabian, P., and Häberle, K. H.: Enhanced ozone strongly reduces carbon sink strength of adult beech (*Fagus sylvatica*) – Resume from the free-air fumigation study at Kranzberg Forest, Environ. Poll., 158, 2527–2532, 2010b.
McLaughlin, S. B., Nosal, M., Wullschleger, S. D., and Sun, G.: Interactive effects of ozone and climate on tree growth and water use in a southern Appalachian forest in the USA, New Phytol., 174, 109–124, 2007a.
McLaughlin, S.B., Wullschleger, S.D., Sun, G., and Nosal, M.: Interactive effects of ozone and climate on water use, soil moisture content and streamflow in a southern Appalachian forest in the USA, New Phytol., 174, 125–136, 2007b.
Mencuccini, M. and Grace, J.: Hydraulic conductance, light interception and needle nutrient concentration in Scots pine stands and their relations with net primary productivity, Tree Physiol., 16, 459–468, 1996.
Mills, G., Hayes, F., Wilkinson, S., and Davies, W. J.: Chronic exposure to increasing background ozone impairs stomatal functioning in grassland species, Glob. Change Biol., 15, 1522–1533, 2009.
Mills, G., Hayes, F., Simpson, D., Emberson, L., Norris, D., Harmens, H., and Büker, P.: Evidence of wide-spread effects of ozone on crops and (semi-)natural vegetation in Europe

ACPD
11, 33583–33650, 2011

(1990–2006) in relation to AOT40- and flux-based risk maps, Glob. Change Biol., 17, 592–613, 2011.
Mills, G., Pleijel, H., Braun, S., Büker, P., Bermejo, V., Calvo, E., Danielsson, H., Emberson, L., Grünhage, L., Fernández, I. G., Harmens, H., Hayes, F., Karlsson, P.-E., and Simpson, D.: New stomatal flux-based critical levels for ozone effects on vegetation, Atmos. Environ., 45, 5064–5068, 2011.
Mintz, Y. and Walker, G. K.: Global fields of soil-moisture and land-surface evapotranspiration derived from observed precipitation and surface air-temperature, J. Appl. Meteor., 32, 1305–1334, 1993.
Monteith, J. L.: Evaporation and Environment, Symp. Soc. Exp. Biol., 19, 205–234, 1965.
Musselman, R. C., Lefohn, A. S., Massman, W. J., and Heath, R. L.: A critical review and analysis of the use of exposure- and flux-based ozone indices for predicting vegetation effects, Atmos. Environ., 40, 1869–1888, 2006.
Norman, J. M.: Simulation of micro-climates, in: Biometeorology in integrated pest management, edited by: Hatfield, J. L. and Thompson, I. J., 65–99, Academic Press, New York, USA, 1982.
Novak, K., Schaub, M., Fuhrer, J., Skelly, J.M., Hug, C., Landolt, W., Bleuler, P., and Kräuchi, N.: Seasonal trends in reduced leaf gas exchange and ozone-induced foliar injury in three ozone sensitive woody plant species, Environ. Poll., 136, 33–45, 2005.
Novak, K., Cherubini, P., Saurer, M., Fuhrer, J., Skelly, J.M., Kräuchi, N., and Schaub, M.: Ozone air pollution effects on tree-ring growth, delta13C, visible foliar injury and leaf gas exchange in three ozone-sensitive woody plant species, Tree Physiol., 27, 941–949, 2007.
Nunn, A., Kozovits, A. R., Reiter, I. M., Heerdt, C., Leuchner, M., Lütz., C., Liu, X., Löw, M., Winkler, J. B., Grams, T. E. E., Häberle, K.-H., Werner, H., Fabian, P., Rennenberg, H., and Matyssek, R.: Comparison of ozone uptake and sensitivity between a phytotron study with young beech and a field experiment with adult beech (*Fagus sylvatica*), Environ. Poll., 137, 494–506, 2005.
Nunn, A. J., Wieser, G., Metzger, U., Löw, M., Wipfler, P., Häberle, K.-H., and Matyssek, R.: Exemplifying whole-plant ozone uptake in adult forest trees of contrasting species and site conditions, Environ. Poll., 146, 629–639, 2007.
Nunn, A. J., Cieslik, S., Metzger, U., Wieser, G., and Matyssek, R.: Combining sap flow and eddy covariance approaches to derive stomatal and non-stomatal O_3 fluxes in a forest stand, Environ. Poll., 158, 2014–2022, 2010.

ACPD
11, 33583–33650, 2011

Ogaya, R. and Peñuelas, J.: Tree growth, mortality, and above-ground biomass accumulation in a holm oak forest under a five-year experimental field drought, Plant Ecol., 189, 291–299, 2007.

Peltzer, D. and Polle, A.: Diurnal fluctuations of antioxidative systems in leaves of field-grown beech trees (*Fagus sylvatica*): responses to light and temperature, Physiol. Plant., 111, 158–164, 2001.

Picon, C., Guehl, J. M., and Ferhi, A.: Leaf gas exchange and carbon isotope composition responses to drought in a drought-avoiding (*Pinus pinaster*) and a drought-tolerant (*Quercus petraea*) species under present and elevated atmospheric CO_2 concentrations, Plant Cell Environ., 19, 182–190, 1996.

Pleijel, H., Danielsson, H., Emberson, L., Ashmore, M.R., and Mills, G.: Ozone risk assessment for agricultural crops in Europe: Further development of stomatal flux and flux-response relationships for European wheat and potato, Atmos. Environ., 41, 3022–3044, 2007.

Rambal, S.: The differential role of mechanisms for drought resistance in a Mediterranean evergreen shrub: a simulation approach, Plant Cell Environ., 16, 35–44, 1993.

Rhea, L. K.: Implications of elevated atmospheric carbon dioxide and tropospheric ozone for water use in stands of trembling aspen and paper birch, doctoral dissertation, Department of Forestry and Environmental Resources, North Carolina State University, 227 pp., 2010.

Ribas, À., Peñuelas, J., Elvira, S., and Gimeno, B. S.: Contrasting effects of ozone under different water supplies in two Mediterranean tree species, Atmos. Environ., 39, 685–693, 2005.

Sala, A. and Tenhunen, J. D.: Site-specific water relations and stomatal response of *Quercus ilex* in a Mediterranean watershed, Tree Physiol., 14, 601–617, 1994.

Saliendra, N. Z., Sperry, J. S., and Comstock, J. P.: Influence of leaf water status on stomatal response to humidity, hydraulic conductance, and soil drought in *Betula occidentalis*, Planta, 196, 357–366, 1995.

Saxton, K. E., Rawls, W. J., Romberger, J. S., and Papendick, R. I.: Estimating generalized soil-water characteristics from texture, Soil Sci. Soc. Am., 50, 1031–1036, 1986.

Schaub, M., Calatayud, V., Ferretti, M., Brunialti, G., Lövblad, G., Krause, G., and Sanz, M. J.: Monitoring of Ozone Injury, Manual Part X, 22 pp., in: Manual on methods and criteria for harmonized sampling, assessment, monitoring and analysis of the effects of air pollution on forests, UNECE ICP Forests Programme Co-ordinating Centre, Hamburg, Germany, (http://www.icp-forests.org/Manual.htm), 2010.

ACPD

11, 33583–33650, 2011

Schupp, R. and Rennenberg, H.: Diurnal changes in the glutathione content of spruce needles (Picea abies L.), Plant Sci., 57, 113–117, 1988.
Schwalm, C. R. and Ek, A. R.: A process-based model of forest ecosystems driven by meteorology, Ecol. Model., 179, 317–348, 2004.
Sellers, P. J., Randall, D. A., Collatz, G. J., Berry, J. A., Field, C. B., Dazlich, D. A., Zhang, C., Collelo, G. D., and Bounoua, L.: A revised land surface parameterization (SiB2) for atmospheric GCMs. 1. Model formulation, J. Climate, 9, 676–705, 1996.
Sellin, A.: Does pre-dawn water potential reflect conditions of equilibrium in plant and soil water status?, Acta Oecologia, 20, 51–59, 1999.
Shuttleworth, W. J. and Wallace, J. S.: Evaporation from sparse crops – an energy combination theory, Quart. J. R. Meteor. Soc., 111, 839–855, 1985.
Simpson, D. and Emberson, L.: Chapter 5. Ozone fluxes – Updates, in: EMEP Status Report 1/06, Transboundary acidification, eutrophication and ground level ozone in Europe since 1990 to 2004, EMEP Status Report 2006 to support the Review of Gothenburg Protocol, Joint MSC-W & CCC & ICP-FORESTs & ICP-M&M & ETC/ACC Report, 2006.
Simpson, D., Fagerli, H., Jonson, J. E., Tsyro, S., Wind, P., and Tuovinen, J.-P.: Transboundary acidification, eutrophication and ground level ozone in Europe, Part I. Unified EMEP model description, EMEP Status Report 1/2003, Norwegian Meteorological Institute, Oslo, 74 pp. + App., http://www.emep.it, 2003a.
Simpson, D., Tuovinen, J.-P., Emberson, L., and Ashmore, M. R.: Characteristics of an ozone deposition module, II: Sensitivity analysis, Water Air Soil Poll., 143, 123–137, 2003b.
Simpson, D., Emberson, L. D., Ashmore, M. R., and Tuovinen, J.-P.: A comparison of two different approaches for mapping potential ozone damage to vegetation, A model study, Environ. Poll., 146, 715–725, 2007.
Sitch, S., Cox, P. M., Collins, W. J., and Huntingford, C.: Indirect radiative forcing of climate change through ozone effect on land-carbon sink, Nature, 448, 791–794, 2007.
Slatyer, R.O.: Plant-water relationships, Academic Press, London, New York, USA, 1967
Sliggers, S. and Kakebeeke, W. (Eds.): Clearing the air, 25 years of the Convention on Long-range Transboundary Air Pollution. United Nations Economic Commission for Europe, Geneva, 168 pp., http://www.unece.org/env/lrtap, 2004.
Solberg, S., Hov, O., Sovde, A., Isaksen, I.S.A., Coddeville, P., De Backer, H., Forster, C., Orsolini, Y., and Uhse, K.: European surface ozone in the extreme summer 2003, J. Geophys. Res., 113, D07307, doi:10.1029/2007JD009098, 2008.

ACPD
11, 33583–33650, 2011

Sturm, N., Köstner, B., Hartung, W., and Tenhunen, J.D.: Environmental and endogenous controls on leaf- and stand-level water conductance in a Scots pine plantation, Ann. Sci. For., 55, 237–253, 1998.

Tardieu, F. and Davies, W. J.: Integration of hydraulic and chemical signalling in the control of stomatal conductance and water status of droughted plants, Plant Cell Environ., 16, 341–349, 1993.

Tardieu, F. and Simonneau, T.: Variability among species of stomatal control under fluctuating soil water status and evaporative demand: modelling isohydric and anisohydric behaviours, J. Exp. Bot., 49, 419–432, 1998.

Tognetti, R., Johnson, J. D., and Michelozzi, M.: The response of European beech (*Fagus sylvatica* L.) seedlings from two Italian populations to drought and recovery, Trees, 9, 348–354, 1995.

Tognetti, R., Longobucco, A., Miglietta, F., and Raschi, A.: Transpiration and stomatal behaviour of *Quercus ilex* plants during the summer in a Mediterranean carbon dioxide spring, Plant Cell Environ., 21, 613–622, 1998.

Tuovinen, J. P., Ashmore, M. R., Emberson, L. D., and Simpson, D.: Testing and improving the EMEP ozone deposition module, Atmos. Environ., 38, 2373–2386, 2004.

Tuovinen, J.-P., Emberson, L., and Simpson, D.: Modelling ozone fluxes to forests for risk assessment: status and prospects, Ann. For. Sci., 66, 401p1–401p12 , 2009.

Tuzet, A., Perrier, A., and Leuning, R.: A coupled model of stomatal conductance, photosynthesis and transpiration, Plant Cell Environ., 26, 1097–1116, 2003.

Uddling, J., Hall, M., Wallin, G., and Karlsson, P. E.: Measuring and modelling stomata conductance and photosynthesis in mature birch in Sweden, Agric. For. Meteor., 132, 115–131, 2005.

Uddling, J., Teclaw, R. M., Kubiske, M. E., Pregitzer, K. S., and Ellsworth, D. S.: Sap flux in pure aspen and mixed aspen-birch forests exposed to elevated carbon dioxide and ozone, Tree Physiol., 28, 1231–1243, 2008.

Uddling, J., Teclaw, R. M., Pregitzer, K. S., and Ellsworth, D. S.: Leaf and canopy conductance in aspen and aspen-birch forests under free-air enrichment of carbon dioxide and ozone, Tree Physiol., 29, 1367–1380, 2009.

Van den Honert, T. H.: Water transport in plants as a catenary process, Discuss. Faraday Soc., 3, 146–153, 1948.

Van Wijk, M. T., Dekker, S. C., Bouten, W., Bosveld, F. C., Kohsiek, W., Kramer, K., and Mohren,

ACPD

11, 33583–33650, 2011

G. M. J.: Modeling daily gas exchange of a Douglas-fir forest: comparison of three stomatal conductance models with and without a soil water stress function, Tree Physiol., 20, 115–122, 2000.
Vieno, M., Dore, A. J., Stevenson, D. S., Doherty, R., Heal, M. R., Reis, S., Hallsworth, S., Tarrason, L., Wind, P., Fowler, D., Simpson, D., and Sutton, M. A.: Modelling surface ozone during the 2003 heat-wave in the UK, Atmos. Chem. Phys., 10, 7963–7978, doi:10.5194/acp-10-7963-2010, 2010.
Vivin, P., Aussenac, G., and Levy, G.: Differences in drought resistance among 3 deciduous oak species grown in large boxes, Ann. Sci. For., 50, 221–233, 1993.
Wallace, J. S.: Calculating evaporation: resistance to factors, Agric. For. Meteorol., 73, 353–366, 1995.
Wallin, G. and Skärby, L.: The influence of ozone on the stomatal and non-stomatal limitation of photosynthesis in Norway spruce, *Picea abies* (L.) Karst, exposed to soil moisture deficit, Trees, 6, 128–136, 1992.
Warren, J. M., Meinzer, F. C., Brooks, J. R., and Domec, J. C.: Vertical stratification of soil water storage and release dynamics in Pacific Northwest coniferous forests, Agric. For. Meteorol., 130, 39–58, 2005.
Warren, J. M., Meinzer, F. C., Brooks, J. R., Domec, J. C., and Coulombe, R.: Hydraulic redistribution of soil water in two old-growth coniferous forests: quantifying patterns and controls, New Phytol., 173, 753–765, 2007.
Wieser, G. and Havranek, W. H.: Environmental control of ozone uptake in *Larix decidua* Mill.: a comparison between different altitudes, Tree Physiol., 15, 253–258, 1995.
Wieser, G., Tegischer, K., Tausz, M., Häberle, K.-H., Grams, T. E. E., and Matyssek, R.: Age effects on Norway spruce (*Picea abies*) susceptibility to ozone uptake: a novel approach relating stress avoidance to defense, Tree Physiol., 22, 583–590, 2002.
Wieser, G., Matyssek, R., Cieslik, S., Paoletti, E., and Ceulemans, R.: Upscaling ozone flux in forests from leaf to landscape, Ital. J. Agron., 1, 34–41, 2008.
Wilkinson, S. and Davies, W. J.: Ozone suppresses soil drying- and abscisic acid (ABA)-induced stomatal closure via an ethylene-dependent mechanism, Plant Cell Environ., 32, 949–959, 2009.
Wilkinson, S. and Davies, W. J.: Drought, ozone, ABA and ethylene: New insights from cell to plant to community, Plant Cell Env., 33, 510–525, 2010.
Williams, M., Rastetter, E. B., Fernandes, D. N., Goulden, M. L., Wofsy, S. C., Shaver, G. R.,

ACPD
11, 33583–33650, 2011

Melillo, J. M., Munger, J. W., Fan, S.-M., and Nadelhoffer, K. J.: Modelling the soil-plant-atmosphere continuum in a *Quercus-Acer* stand at Harvard Forest: the regulation of stomatal conductance by light, nitrogen and soil/plant hydraulic properties, Plant Cell Environ., 19, 911–927, 1996.

Willmott, C. J.: Some comments on the evaluation of model performance, Bull. Amer. Meteor. Soc., 63, 1309–1313, 1982.

Zhang, X., Friedl, M. A, Schaaf, C. B., and Strahler, A. H.: Climate controls on vegetation phenological patterns in northern mid- and high latitudes inferred from MODIS data, Glob. Change Biol., 10, 1133–1145, 2004.

Zweifel, R., Zimmermann, L., and Newbery, D.M.: Modeling tree water deficit from microclimate: an approach to quantifying drought stress, Tree Physiol., 25, 147–156, 2005.

ACPD

11, 33583–33650, 2011

Table 1. Symbols, abbreviations and parameter values.

Symbol		Parameter value	Units
a	Plant absorption flux		$m\,s^{-1}$
b	Texture dependent soil conductivity parameter		–
C	Plant capacitance	1 (B/T), 0.17 (M)	$mm\,MPa^{-1}$
C_c	Coefficient of transpiration fraction of E_{at}		–
c_p	Specific heat of air		$J\,kg^{-1}\,K^{-1}$
C_s	Coefficient of evaporation fraction of E_{at}		–
d	Soil measurement depth		m
D	Vapour pressure deficit of air		kPa
d_r	Root zone depth		m
FC	θ at field capacity		$m^3\,m^{-3}$
PAW_{min}	θ at Ψ_{min}		$m^3\,m^{-3}$
E_{at}	Total evapotranspiration		$m\,day^{-1}$
E_i	Evaporation from canopy		$m\,day^{-1}$
E_s	Soil surface evaporation		$m\,day^{-1}$
E_t	Plant transpiration		$m\,day^{-1}$
G	Soil surface heat flux		$W\,m^{-2}$
I_{dir}	Direct sunlight		$W\,m^{-2}$
I_{diff}	Diffuse sunlight		$W\,m^{-2}$
K_s	Soil hydraulic conductivity		$m\,s^{-1}$
K_{sat}	Soil hydraulic conductivity at saturation		$m\,s^{-1}$
k_1	Root density parameter	3.5×10^{-12}	$m\,s^{-1}$
LAI	(Projected) Leaf area index		$m^2\,m^{-2}$
PAW	Plant available soil water		m
P_{input}	Precipitation reaching the soil surface		m
P_{total}	Total precipitation		m
q	Storage/destorage flux		$m\,s^{-1}$
r_{sto}	Stomatal resistance (leaf-level)		$m\,s^{-1}$
r_{ext}	External plant surface resistance (leaf-level)		$m\,s^{-1}$

ACPD
11, 33583–33650, 2011

Table 1. Continued.

R_a	Aerodynamic resistance		$m\,s^{-1}$
R_b	Boundary layer resistance		$m\,s^{-1}$
R_{bH_2O}	Boundary layer resistance to water vapour exchange		$m\,s^{-1}$
R_c	Storage hydraulic resistance	0.4 (B/T), 2 (M)	$MPa\,h\,mm^{-1}$
R_{gs}	Soil resistance to ozone		$m\,s^{-1}$
R_{stoH_2O}	Stomatal resistance to water vapour exchange		$m\,s^{-1}$
R_{inc}	In canopy resistance		$m\,s^{-1}$
R_p	Plant hydraulic resistance	5.3 (B/T), 7 (M)	$MPa\,h\,mm^{-1}$
R_{sp}	Soil-plant hydraulic resistance		$MPa\,h\,mm^{-1}$
R_{sr}	Soil-root hydraulic resistance		$MPa\,h\,mm^{-1}$
R_{soil}	Soil resistance to water vapour		$m\,s^{-1}$
SAI	Surface area index		$m^2\,m^{-2}$
S_c	Canopy storage capacity		m
S_n	Soil water storage		m
S_{n-1}	Soil water storage of previous day		m
β	Root fraction parameter	0.97	
T	Air temperature		°C
Δ	Slope of the relationship between saturation vapour pressure and temperature		$MPa\,K^{-1}$
γ	Psychrometric constant		$MPa\,K^{-1}$
λ	Latent heat of vaporisation		$J\,kg^{-1}$
ρ_a	Air density		$kg\,m^{-3}$
θ	Volumetric soil water content		$m^3\,m^{-3}$
θ_{sat}	Volumetric soil water content at saturation		$m^3\,m^{-3}$
Φ_n	Net radiation at top of canopy		$W\,m^{-2}$

ACPD
11, 33583–33650, 2011

Table 1. Continued.

Φ_{ns}	Net radiation at soil surface	$W\,m^{-2}$
Ψ_e	Soil water potential at air entry	MPa
Ψ_{leaf}	Leaf water potential	MPa
$\Psi_{leaf,pd}$	Pre-dawn leaf water potential	
Ψ_{min}	Soil water potential below which plant water uptake ceases	MPa
Ψ_r	Reservoir potential	MPa
Ψ_{sat}	Soil water potential at saturation	MPa
Ψ_{soil}	Soil water potential	MPa

N.B. B/T = boreal/temperate forest trees; M = Mediterranean forest trees.

ACPD
11, 33583–33650, 2011

Table 2. DO_3SE model parameterisation used for each dataset.

Site name	Country	Species	g_{max} (mmol O_3 m^{-2} PLA s^{-1})	LAI_{min}, LAI_{max}	Light factor, α	T_{min}, T_{opt}, T_{max} (°C)	D_{min}, D_{max} (kPa)	Soil texture curve constants *FC*, Ψ_e, *b*, K_{sat}	Root depth (soil depth) (m)	Canopy height (m)	References
Asa	Sweden	Norway spruce	112	6.5, 6.5	0.006	*0, 20, 35*	0.8, 2.8	*0.26, −0.00158, 4.38, 0.0002178 (Silt loam)*	0.4	20	Karlsson et al. (2006)
Davos	Switzerland	Norway spruce	125	3.9, 3.9	0.01	*0, 20, 35*	0.5, 3.0	0.29, −0.00158, 4.38, 0.00002178 (Silt loam)	1.0	20	Zweifel et al. (2005)
Forellenbach	Germany	Beech	150	0, 5.0	0.006	5, 16, 33	1.0, 3.1	*0.29, −0.00158, 4.38, 0.0009576 (Silt loam)*	0.9	25	Baumgarten et al. (2000)
Hortenkopf	Germany	Beech (20 %)	150 [214]	0, 6.0	0.003	0, 20, 35	1.0, 3.25	*0.22, −0.00091, 3.31, 0.0009576 (Sandy/silt loam)*	0.8–1.2	22 [28]	Werner (unpublished)
		Oak (80 %)	230 [214]							30 [28]	
Kranzberger Forst	Germany	Beech	148	0, 5.6	0.006	8, 21, 34	1.1, 3.1	0.38, −0.00588, 7.0, 0.00016 (Silt/Clay loam)	0.8	23	Nunn et al. (2005, 2007), Raspe (personal communication, ▲ *yew*)
Miraflores de la Sierra	Spain	Holm oak	180	1, 2.5	0.003	6, 19, 32	1.3, 3.8	0.27, −0.00158, 4.38, 0.0002178 (Sandy/silt loam)	1.5	6	Alonso et al. (2008)
Norunda	Sweden	Norway spruce (33 %)	35 [115]	7.1, 7.1 [4.7]	0.006	*0, 20, 35*	0.8, 2.8	0.3, −0.005, 2.8, 0.0006576 (Sandy loam)	0.5	19 [17]	Lagergren et al. (2008)
		Scots pine (64 %)	160 [115]	3.7, 3.7 [4.7]						19 [17]	
Prades	Spain	Holm oak	100	2.5, 4.0	0.012	*1, 23, 39*	2.2, 4.0	*0.37, −0.00588, 7, 0.00016(Clay loam)*	1.5 (0.9)	4	Ogaya and Peñuelas (2007)
Rhinelander	USA	Aspen	135	0, 3.6	*5, 16, 33*	1.0, 3.1	0.16, −0.00085, 3.25, 0.0009576 (Sandy loam)	0.65	7–8 [7.5]		King et al. (2005), Uddling et al. (2008, 2009), Rhea et al. (2010)
		Aspen-Birch mixture	116	0, 4.4							
Strawberry Peak/Crestline	USA	Evergreen oak (*Quercus spp.*)	180	3.5, 5	0.012	*1, 23, 39*	2.2, 4.0	*0.26, −0.00188, 6.58, 0.0002286 (Loam)*	4(4)	15	Grulke (unpublished)

N.B. Default values based on UNECE (2004) indicated in italics. For mixed canopies, weighted means for g_{max}, LAI and canopy height are used and provided in square brackets; percent coverage of species given in brackets in species column. PLA = Projected leaf area. The formulation of the functions used to define LAI, f_{light}, f_{temp} and f_{VPD} are described in LRTAP Convention, 2010; the *α*, *min*, *opt* and *max* values describe the specific parameters for the respective function.

ACPD
11, 33583–33650, 2011

Table 3. Water holding characteristics of four soil texture classes, after Tuzet et al. (2003).

Soil texture	Soil texture classification	FC, $m^3\ m^{-3}$	Ψ_e MPa	b	K_{sat}
Sandy loam	Coarse	0.16	−0.00091	3.31	9.576×10^{-4}
Silt loam	Medium coarse	0.26	−0.00158	4.38	2.178×10^{-4}
Loam	Medium	0.29	−0.00188	6.58	2.286×10^{-4}
Clay loam	Fine	0.37	−0.00588	7	1.6×10^{-4}

ACPD
11, 33583–33650, 2011

Table 4. Forest datasets used to test soil water status estimates of the DO_3SE model. References as in Table 2.

Site name	Country	Location	Elevation (m a.s.l.)	Species	Wind speed height (m)	Soil texture	Soil water metric	Soil water measurement depth (m)	g_{sto} data	Measurement period
Asa	Sweden	57°09′ N 14°45′ E	285	Norway spruce	5	Silt loam	Ψ_{soil} (MPa)	0.4	–	1995, 2000
Davos	Switzerland	46°48′ N 09°51′ E	1640	Norway spruce	30	Silt loam	Ψ_{soil} (MPa)	0.1	–	2004
Forellenbach	Germany	48°56′ N 13°25′ E	825	Beech	51	Sandy loam	PAW (mm)	1.2	–	2003
Hortenkopf	Germany	49° 16′ N 07°49′ E	550	Beech and oak	10	Sandy loam	θ (%)	0.4	–	2000–2003
Kranzberger Forst	Germany	48°25′ N 11°25′ E	485	Beech	33	Silt/Clay loam	θ (%)	0.3	Porometer	2003
Miraflores de la Sierra	Spain	40°48′ N 03°48′ W	1095	Holm oak	10	Sandy/silt loam	Ψ_{pdleaf} (MPa)	–	LI-COR 6400	2004, 2005
Norunda	Sweden	60°05′ N 17°29′ E	45	Norway spruce, Scots pine	37	Sandy loam	θ (%)	0.5	Sap flow	1999
Prades	Spain	41°12′ N 00°55′ E	930	Holm oak	5	Clay loam	θ (%)	0.1, 0.4	–	2001–2003
Rhinelander	USA	45°36′ N 89°30′ W	500	Aspen; mixed Aspen-Birch	10	Sandy loam	θ (%)	Between 0.05 and 1.3	Sap flow	2006
Strawberry Peak/Crestline	USA	34°30′ N 117°18′ W	1800	Evergreen oak (*Quercus spp.*)	15	Loam	θ (%)	0.5	–	1995

Measurement height: OF = Open Field; C = within Canopy

ACPD
11, 33583–33650, 2011

Table 5. Statistical agreement (coefficient of determination (R^2), mean bias (MB; normalised value in parenthesis), root mean square error (RMSE; normalised value in parenthesis) and Willmott's index of agreement (IA)) of measured and modelled soil water using four methods that relate soil water to g_{sto}. Results for Miraflores are not shown due to scarcity of measured data points. Metric units: Ψ_{soil} [MPa], PAW [mm], θ[%].

Site	Year	Soil water	f_{SWP}				f_{PAW}				SS				NSS			
		Metric	R^2	MB (NMB)	RMSE (NRMSE)	IA	R^2	MB (NMB)	RMSE (NRMSE)	IA	R^2	MB (NMB)	RMSE (NRMSE)	IA	R^2	MB (NMB)	RMSE (NRMSE)	IA
Asa	1995	Ψ_{soil}	0.48	−0.03 (14.02)	0.53 (−236.25)	0.69	0.47	0.05 (−24.41)	0.33 (−145.83)	0.79	0.57	0.20 (−90.32)	0.36 (−161.98)	0.44	0.51	0.19 (−83.15)	0.33 (−148.37)	0.50
	2000		0.02	0.02 (−54.89)	0.02 (−62.87)	0.19	0.02	0.02 (−54.89)	0.02 (−62.87)	0.19	0.04	0.02 (−64.86)	0.02 (−65.74)	0.18	0.03	0.02 (−61.43)	0.02 (−63.04)	0.19
Davos	2004	Ψ_{soil}	0.01	0.01 (−42.73)	0.01 (−56.79)	0.44	0.00	0.01 (−45.07)	0.01 (−58.54)	0.43	0.00	0.01 (−48.10)	0.01 (−60.67)	0.42	0.00	0.01 (−44.07)	0.01 (−57.87)	0.43
Forellenbach	2003	PAW	0.91	21.00 (29.98)	25.43 (36.32)	0.88	0.90	14.49 (20.69)	24.28 (34.67)	0.90	0.08	109.50 (156.34)	113.53 (162.09)	0.31	0.61	78.29 (111.78)	80.62 (115.11)	0.44
Hortenkopf	2000	θ	0.78	0.01 (7.40)	0.02 (9.15)	0.84	0.78	0.01 (7.40)	0.02 (9.15)	0.84	0.40	0.03 (15.59)	0.03 (17.98)	0.49	0.54	0.03 (14.13)	0.03 (16.19)	0.53
	2001		0.81	-0.02 (−16.67)	0.03 (23.31)	0.90	0.81	0.01 (4.46)	0.02 (17.00)	0.94	0.55	0.09 (74.40)	0.10 (80.67)	0.42	0.88	0.07 (57.97)	0.07 (60.98)	0.56
	2002		0.60	-0.03 (−24.91)	0.03 (27.88)	0.61	0.12	0.00 (-0.73)	0.02 (20.73)	0.59	0.00	0.09 (84.57)	0.09 (90.61)	0.25	0.04	0.05 (45.96)	0.05 (51.67)	0.39
	2003		0.94	-0.01 (−5.50)	0.02 (18.20)	0.97	0.94	0.00 (3.42)	0.01 (13.21)	0.98	0.73	0.07 (60.88)	0.08 (67.36)	0.58	0.83	0.03 (30.67)	0.04 (35.72)	0.84
Kranzberger Forst	2003	θ	0.84	-0.02 (−7.18)	0.04 (12.01)	0.92	0.85	-0.02 (−8.19)	0.04 (12.41)	0.91	0.43	0.03 (8.84)	0.05 (16.53)	0.73	0.73	0.00 (0.63)	0.03 (9.87)	0.92
Norunda	1999	θ	0.89	-0.02 (−12.67)	0.03 (22.52)	0.96	0.89	-0.01 (−5.97)	0.03 (18.83)	0.97	0.87	0.05 (29.84)	0.06 (38.03)	0.85	0.94	0.01 (4.78)	0.02 (14.84)	0.98
Prades	2001–2003	θ	0.77	-0.03 (−13.57)	0.05 (19.24)	0.88	0.82	-0.03 (−9.82)	0.04 (15.12)	0.92	0.84	-0.02 (−6.78)	0.03 (12.49)	0.94	0.81	-0.02 (−9.73)	0.04 (15.34)	0.92
Rhinelander	2003	θ	0.72	0.00 (-0.56)	0.03 (19.41)	0.91	0.53	-0.01 (−9.53)	0.03 (26.80)	0.83	0.27	0.01 (4.69)	0.04 (31.56)	0.68	0.41	0.00 (-0.76)	0.04 (28.07)	0.78
Strawberry Peak/Crestline	1995	θ	0.78	0.03 (18.70)	0.04 (25.74)	0.86	0.80	0.03 (19.40)	0.04 (25.84)	0.86	0.89	0.06 (41.61)	0.06 (44.09)	0.70	0.90	0.05 (36.34)	0.05 (38.73)	0.75

ACPD
11, 33583–33650, 2011

Table 6. Modelled length and severity of the drought stress period affecting g_{sto} for all sites. f_{SW} <1 and $f_{SW\ min}$ indicate the total days of water stress when $\Psi_{soil} < \Psi_{max}$ and when $\Psi_{soil} < \Psi_{min}$, respectively.

Model		f_{SWP}				f_{PAW}				SS				NSS			
		$f_{SW} < 1$		f_{SWmin}		$f_{SW} < 1$		f_{SWmin}		$f_{SW} < 1$		f_{SWmin}		$f_{SW} < 1$		f_{SWmin}	
Site	Year	No. of days	% of total days	No. of days	% of total days	No. of days	% of total days	No. of days	% of total days	No. of days	% of total days	No. of days	% of total days	No. of days	% of total days	No. of days	% of total days
Asa	1995	34	13.9	5	2.0	45	18.4	0	0	0	0	0	0	7	2.9	0	0
	2000	0	0	0	0	0	0	0	0	0	0	0	0	0	0	0	0
Davos	2004	0	0	0	0	0	0	0	0	0	0	0	0	0	0	0	0
Forellenbach	2003	63	17.3	0	0	98	26.8	0	0	0	0	0	0	0	0	0	0
Hortenkopf	2000	0	0	0	0	0	0	0	0	0	0	0	0	0	0	0	0
	2001	40	21.9	0	0	88	48.1	0	0	0	0	0	0	0	0	0	0
	2002	59	32.2	0	0	106	57.9	0	0	0	0	0	0	0	0	0	0
	2003	91	49.7	3	1.6	113	61.7	0	0	0	0	0	0	4	2.2	0	0
Kranzberger Forst	2003	108	29.6	3	0.8	164	44.9	4	1.1	0	0	0	0	57	15.6	0	0
Miraflores	2004/2005	291	39.8	124	17.0	307	42.0	51	7.0	228	31.2	101	13.8	253	34.6	104	14.2
Norunda	1999	97	49.0	14	7.1	120	60.6	1	0.5	0	0	0	0	70	35.4	0	0
Prades	2001–2003	455	43.8	96	9.2	870	83.8	55	5.3	266	25.1	16	1.5	328	31.6	22	2.1
Rhinelander	2006	38	13.2	9	3.1	86	29.8	8	2.8	13	4.5	0	0	28	9.7	5	1.7
Strawberry Peak/Crestline	1995	200	54.8	146	40	212	58.1	142	38.9	150	41.1	65	17.8	161	44.1	89	24.4

ACPD
11, 33583–33650, 2011

Table 7. Effects on changing parameters soil texture, g_{max}, LAI and root depth on POD_1 and number of days with $f_{SW} < 1$, therefore indicating drought conditions at Norunda 1999. Percentage change of POD_1 as compared to initial parameterisation (=sandy loam) indicated in brackets. The sandy loam soil texture parameterisation represents the original parameterisation used in model runs (Tables 3 and 4).

Parameter	Value	POD_1 (mmol O_3 m^{-2})	f_{SW} <1 (days)	POD_1 (mmol O_3 m^{-2})	f_{SW} < 1 (days)
Model		f_{SWP}		f_{PAW}	
Soil texture	Sandy loam	4.64	97	4.09	120
	Clay loam	3.19 (−31)	116	3.56 (−13)	122
g_{max} (mmol m^{-2} s^{-1})	85	3.37 (−27)	79	3.11 (−24)	108
	145	5.52 (+19)	106	5.07 (+24)	131
LAI	3.5	4.70 (+1)	96	4.53 (+11)	119
	5.9	4.74 (+2)	96	4.05 (−1)	120
Root depth	0.38	3.92 (−16)	104	3.43 (−16)	124
(m)	0.63	5.25 (+13)	84	4.96 (+21)	120
		SS		NSS	
Soil texture	Sandy loam	2.79	0	3.93	70
	Clay loam	2.12 (−24)	59	2.88 (−27)	89
g_{max}	85	1.50 (−46)	0	2.91 (−26)	18
(mmol m^{-2} s^{-1})	145	3.77 (+35)	36	4.71 (+20)	79
LAI	3.5	2.51 (−10)	14	3.78 (−4)	74
	5.9	3.03 (+9)	0	4.26 (+8)	61
Root depth	0.38	2.37 (−15)	38	3.32 (−16)	72
(m)	0.63	2.91 (+4)	0	4.79 (+22)	26

ACPD
11, 33583–33650, 2011

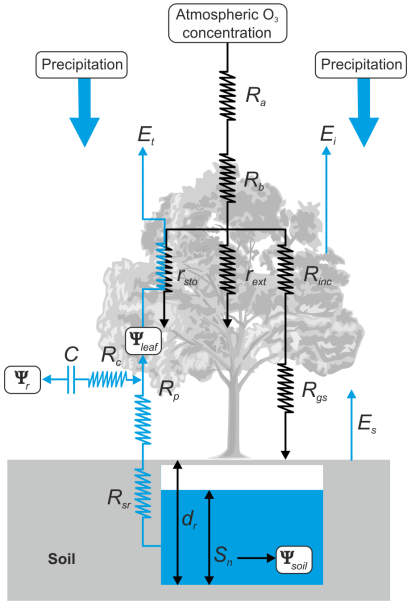

Fig. 1. Schematic of resistance to O_3 deposition (black) and water vapour exchange (blue) in relation to the DO_3SE model resistance scheme. The coupling between soil water loss and transpiration is achieved through the influence of soil drying on g_{sto} resulting in reduced transpiration. Denotation: see Table 1. Note that all possible resistances are shown in the schematic though different models will use different combinations of these resistances; the *Rsr* and *Rp* terms are specific to the SS model and the *Rsr*, *Rp*, *Rc* and *C* terms are specific to the NSS model. The f_{SWP} and and f_{PAW} models do not use these particular terms. Further details are provided in the text.

ACPD
11, 33583–33650, 2011

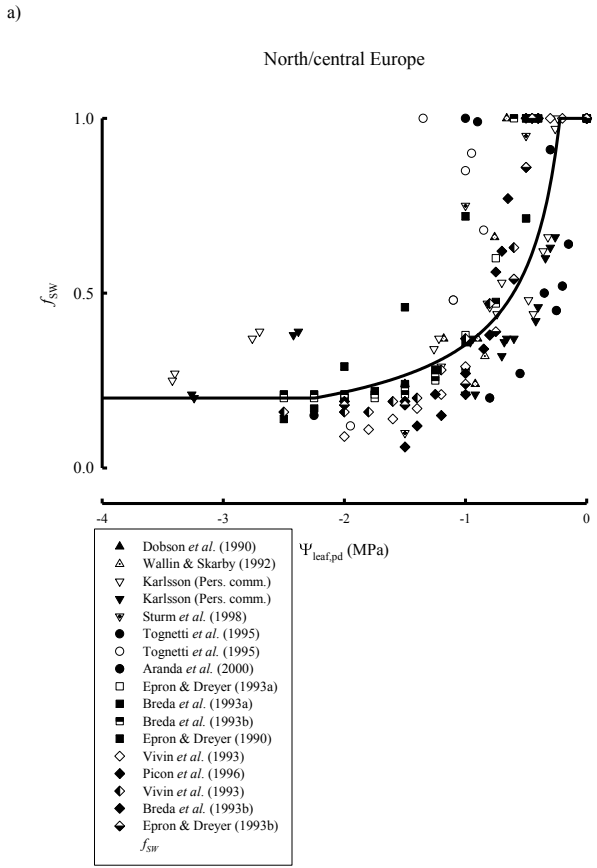

Fig. 2a. f_{SW} relationships in comparison with observed data describing relative *g* with pre-dawn leaf water potential for **(a)** coniferous (Norway spruce and Scots pine) and deciduous (beech) trees in north and central Europe with $\Psi_{max} = -0.6$ MPa; $\Psi_{min} = -1.5$ MPa; PWP = -4.0 MPa.

ACPD
11, 33583–33650, 2011

b)

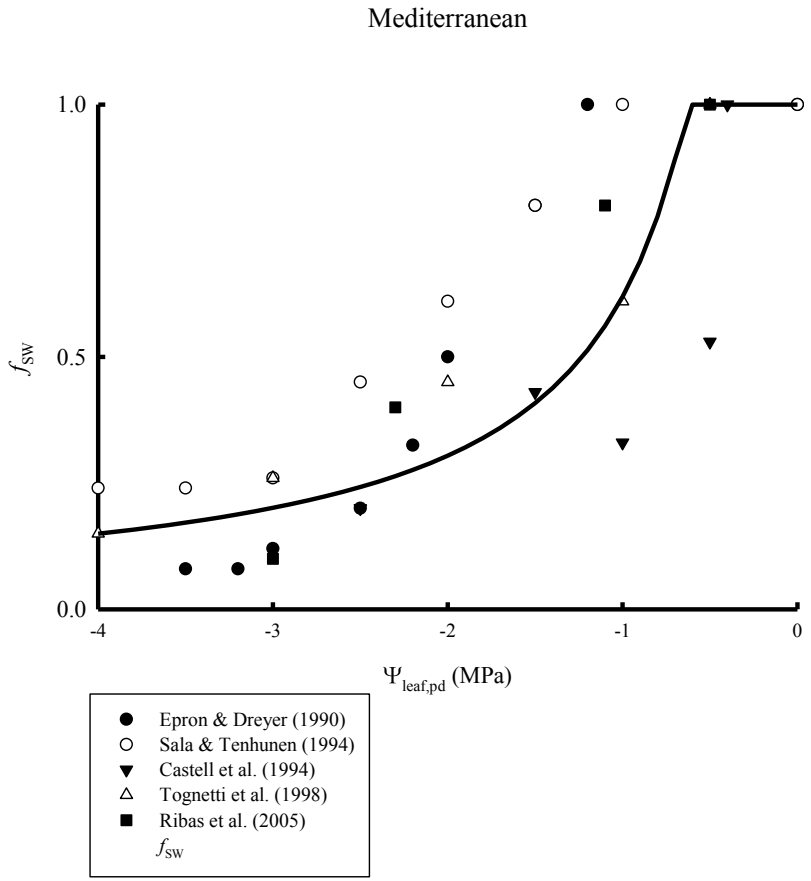

Fig. 2b. f_{SW} relationships in comparison with observed data describing relative g with pre-dawn leaf water potential for **(b)** Mediterranean trees (holm oak) with $\Psi_{max} = -0.9$ MPa; $\Psi_{min} = -3.6$ MPa; PWP = −4.0 MPa.

ACPD
11, 33583–33650, 2011

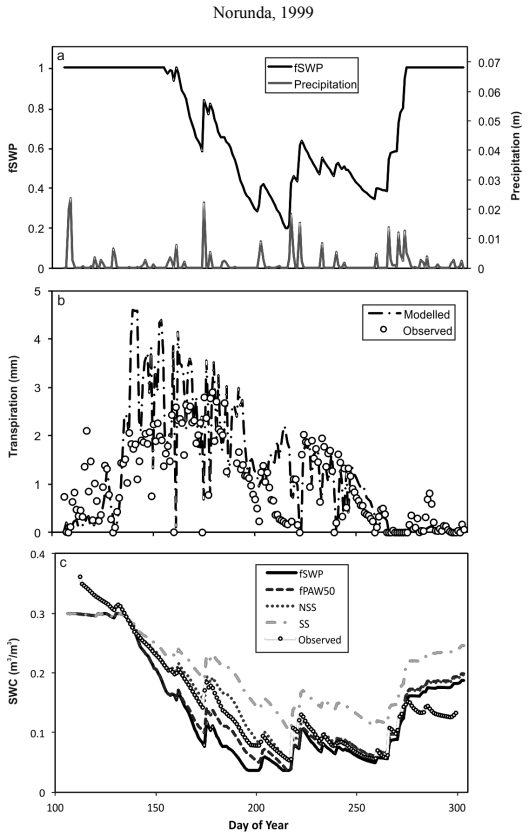

Fig. 3. (a) Modelled f_{SWP} and measured precipitation for a mixed Norway spruce and Scots pine stand at Norunda in 1999 using the f_{PAW} method; **(b)** Observed and modelled transpiration for the same year, stand and soil water calculation method; **(c)** Observed and modelled soil water content (SWC) using all four methods that relate soil water to g_{sto} (see methods section for details).

ACPD
11, 33583–33650, 2011

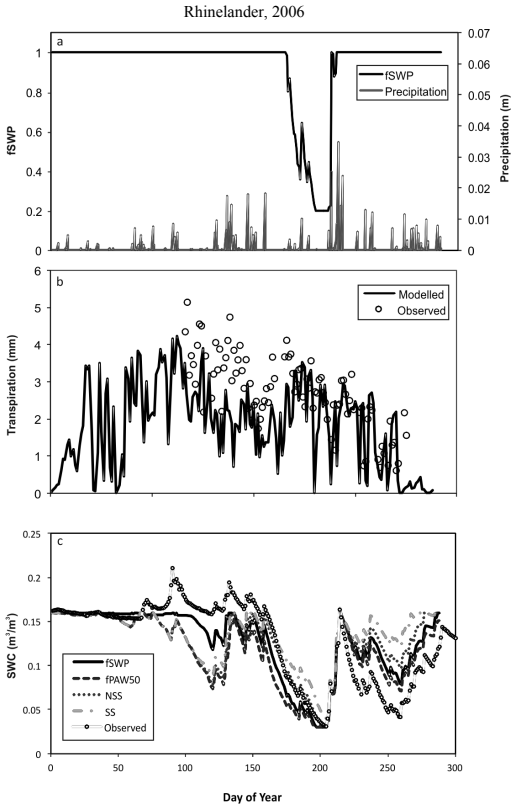

Fig. 4. **(a)** Modelled f_{SWP} and measured precipitation for a mixed aspen-birch stand at Rhinelander in 2006 using the f_{SWP} model; **(b)** Observed and modelled transpiration for the same year, stand and soil water calculation method; **(c)** Observed and modelled soil water content (SWC) using all four methods that relate soil water to g_{sto} (see methods section for details).

ACPD
11, 33583–33650, 2011

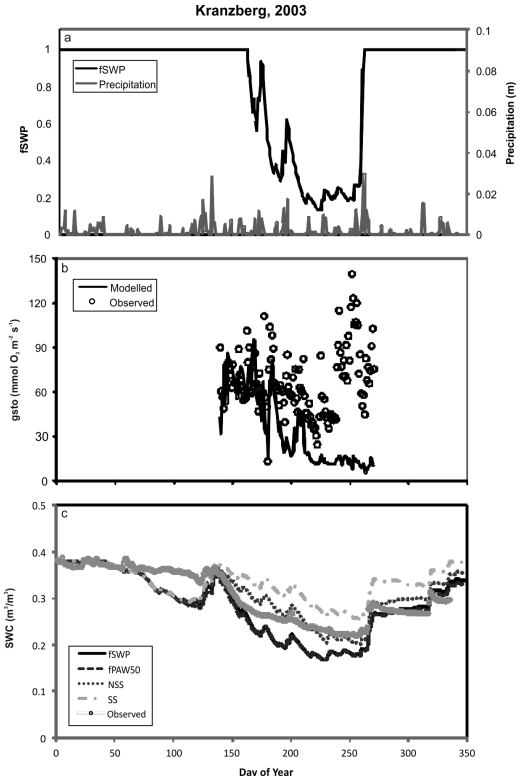

Fig. 5. (a) Precipiation and modelled f_{SWP} for a beech stand at Kranzberger Forst in 2003 using the f_{SWP} model (see methods section for details); **(b)** Observed and modelled leaf-level g_{sto} for the same year, stand and soil water calculation method; **(c)** Observed and modelled soil water content (SWC) using all four methods that relate soil water to g_{sto} (see methods section for details).

ACPD
11, 33583–33650, 2011

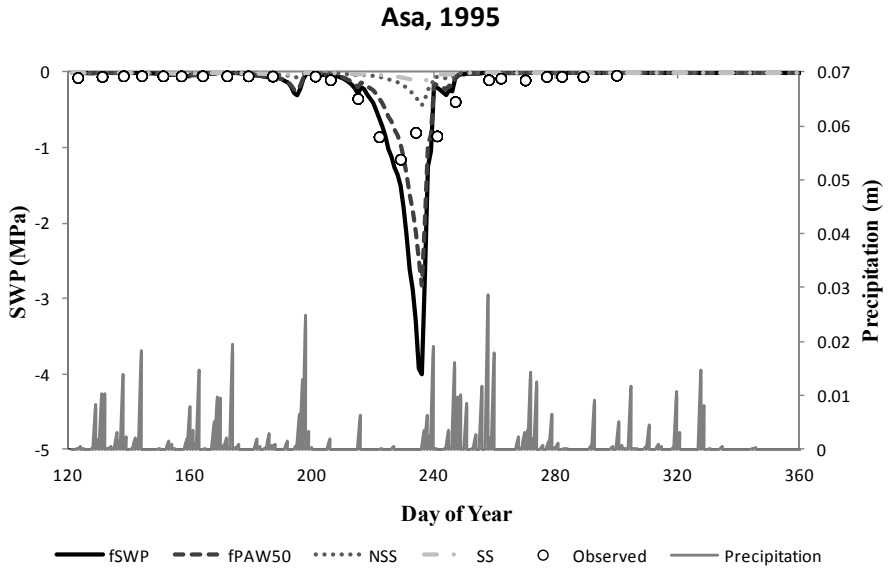

Fig. 6. Comparison of observed and modelled soil water potential (SWP) in 1995 for a Norway spruce stand at Asa using four methods that relate soil water to g_{sto} (see methods section for details).

ACPD
11, 33583–33650, 2011

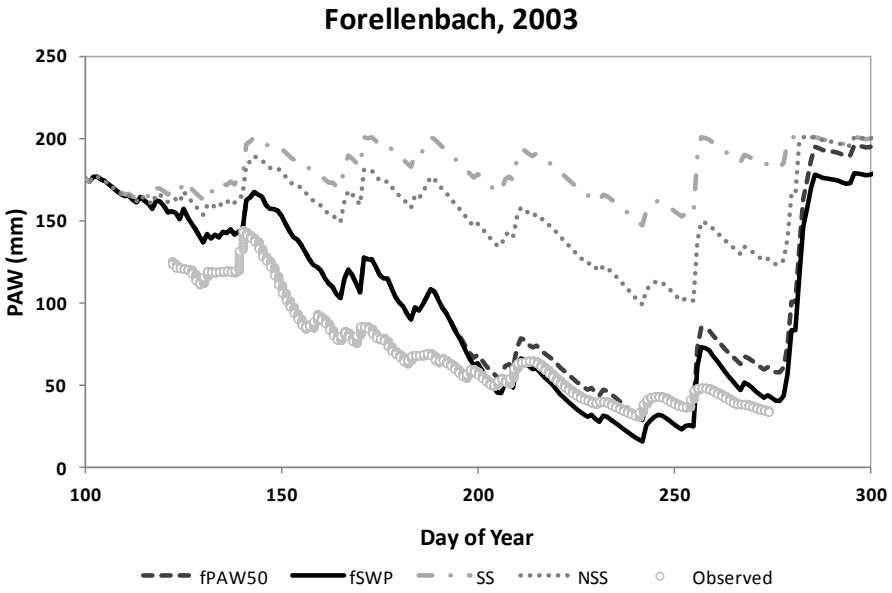

Fig. 7. Comparison of observed and modelled plant available water (PAW) in 2003 for a beech stand at Forellenbach using four methods that relate soil water to g_{sto} (see methods section for details).

ACPD
11, 33583–33650, 2011

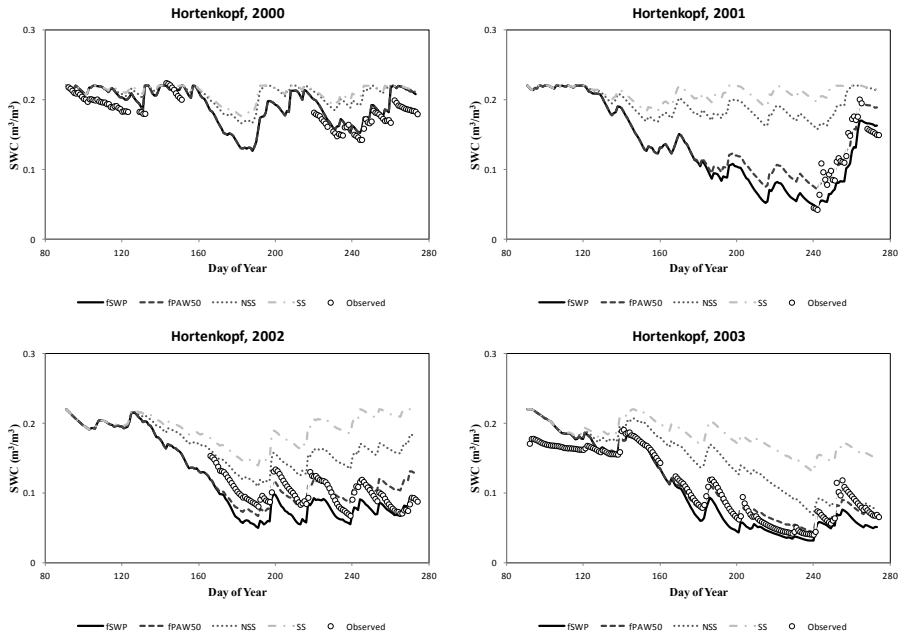

Fig. 8. Comparison of observed and modelled soil water content (SWC) in 2000, 2001, 2002 and 2003 for a mixed beech and temperate oak stand at Hortenkopf using four methods that relate soil water to g_{sto} (see methods section for details).

ACPD
11, 33583–33650, 2011

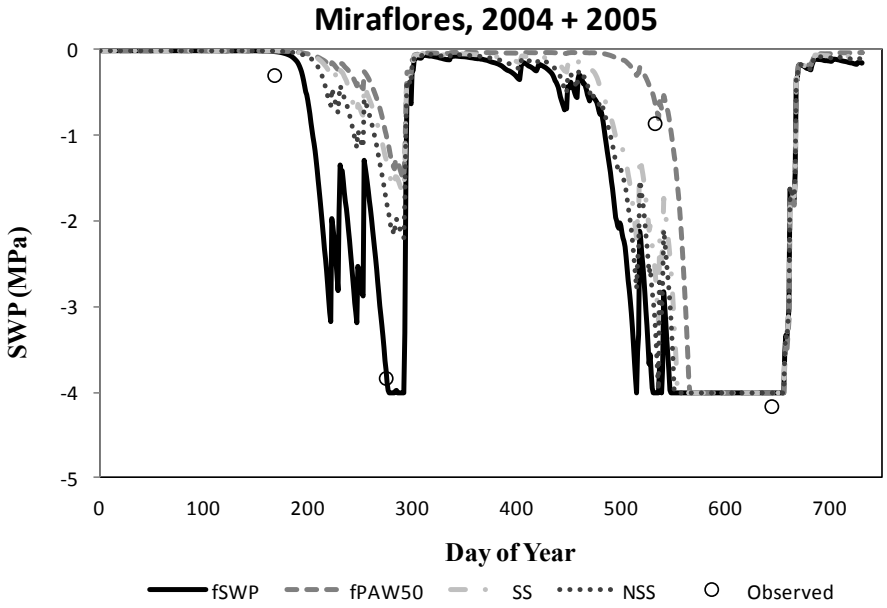

Fig. 9. Comparison of modelled soil water potential (SWP) and observed pre-dawn leaf water potential in 2004 and 2005 for a holm oak stand at Miraflores de la Sierra using four methods that relate soil water to g_{sto} (see methods section for details).

ACPD
11, 33583–33650, 2011

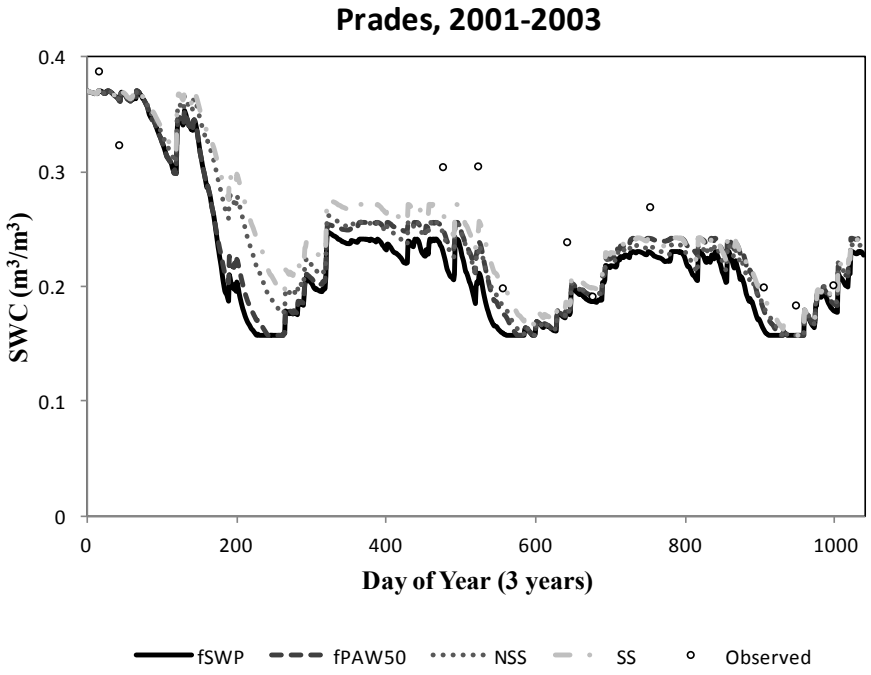

Fig. 10. Comparison of modelled and observed soil water content (SWC) from 2001 to 2003 for a holm oak stand at Prades using 4 methods that relate soil water to g_{sto} (see methods section for details).

ACPD
11, 33583–33650, 2011

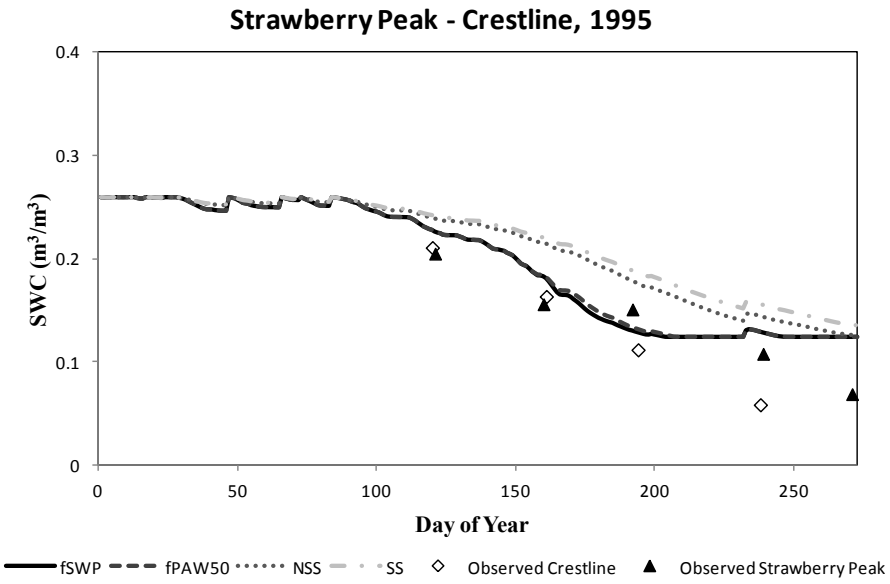

Fig. 11. Comparison of observed and modelled soil water content (SWC) in 1995 for a evergreen oak stand at Strawberry Peak/Crestline using four methods that relate soil water to g_{sto} (see methods section for details).

ACPD
11, 33583–33650, 2011